Nota Resúmen sobre los artículos presentados a efectos de Ascender a Profesor Asociado

Carlos E Cadenas R.
Universidad de Carabobo
Facultad Experimental de Ciencias y Tecnología
e-mail: ccadenas@uc.edu.ve

Resumen

En esta nota se presenta a manera de resúmen, algunas de las actividades realizadas por mi persona y resultados principales relacionados con los artículos (en inglés) presentados para ascender en el escalafón de la Universidad de Carabobo a la categoría de Profesor Asociado. En primera instancia se mencionan las relacionadas con el área de investigación en Métodos Miméticos y luego en el área de Elementos Finitos Mínimos Cuadrados. La mayoría de las fechas mencionadas son aproximadas, y para efectos de comparación de fechas con mi anterior ascenso se tomará en cuenta que la presentación relacionada con el mismo fué en febrero de 2002.

1 Métodos Miméticos

1.1 Actividades Realizadas

A finales de Noviembre de 2001 el Profesor José Castillo realizó una charla en la Universidad Central de Venezuela, relacionada con la obtención de operadores diferenciales (Divergencia y Gradiente) miméticos por medio de métodos matriciales. En dicha metodología se destacaba un procedimiento a partir de las matrices de Vandermonde e identificaban a diversos operadores discretos necesarios para cumplir un teorema de la Divergencia Discreto Generalizado, siempre y cuando se utilicen mallas uniformes. A partir de dicha fecha realicé una recopilación y estudio de artículos relacionados con los métodos de discretización mimética al mismo tiempo que dirigía varios trabajos especiales de grado relacionados con la aplicación de dichos métodos. De uno de estos trabajos de grado luego se hizo un resúmen en 1D que fué publicado en la revista *Ingeniería UC* en el año 2004, véase [1] (los resultados en 2D no han sido publicados). Simultaneamente en el año 2002 trataba de justificar todos los pasos de la metodología de los profesores José Castillo y Grone (posteriormente publicada en 2003, [2]). Sin embargo la justificación de la matriz de Vandermonde para mí no estaba clara, por lo que decidí proponer una metodología para la obtención de dichas matrices para mallas no uniformes, en esta etapa el profesor Orestes Montilla se incorpora a dicha investigación, con lo que publicamos dicha metodología relacionada solamente con el operador de Divergencia en la revista ”Ingeniería UC”en el año 2004, véase [3]. Luego el profesor Orestes Montilla en el año 2004 presenta su trabajo de ascenso relacionado con los avances realizados en proponer una generalización de la metodología del artículo [2], basado en las matrices de Vandermonde Generalizadas tanto para el operador mimético Divergencia como Gradiente sobre mallas no uniformes. Dicha metodología fué mejorada y publicada en el artículo [4] del año 2006. Sobre

esta área de investigación realicé otras investigaciones sobre mallas uniformes para la ecuación de Helmholtz y sobre la ecuación de Sturn Liuville que fueron presentados en dos congresos en los años 2003 y 2005 en San Diego, USA y Granada, España. Estos últimos resultados no han sido publicados.

1.2 Resultado Principal del artículo [3]

En este artículo se introduce la función de prueba $f(x) = (x - x_{j+\frac{1}{2}})^n$ que permite obtener sobre un mallado escalonado no uniforme las entradas de la matriz de Vandermonde que a posteriori puede ser usada para construir el operador de divergencia mimético sobre mallas no uniformes, utilizando el mismo procedimiento dado en [2] para mallas uniformes. Dichas entradas no sería más que los coeficientes de a_{ji} dado en el Teorema 1. Se presentan además dos ejemplos de matrices de Vandermonde: para una malla uniforme y para una malla no uniforme suave.

1.3 Resultados Principales del artículo [4]

En este artículo se usan las funciones de prueba dadas en [3], las cuales se reescriben en la ecuación (4) del artículo [4], para introducir el procedimiento descrito en [3] y así obtener las matrices de Vandermonde que luego se usan para obtener el operador de divergencia mimético. En la sección 3.2 se introducen las funciones de prueba $f_{i,n} = (x - x_i)^n$ (ecuación (16)) que permiten obtener la matriz de Vandermonde que luego son usadas para obtener el operador gradiente mimético para mallas no uniformes. El procedimiento para obtener estos operadores y los otros necesarios para satisfacer un teorema de la divergencia Generalizado, dado por la ecuación (30) es el mismo que el descrito en [2]. Se calculan así todos los operadores involucrados en dicho teorema de la divergencia Generalizado.

2 Métodos de Elementos Finitos Mínimos Cuadrados

Métodos de Elementos Finitos Mínimos Cuadrados

A finales del año 1998 el profesor Vianey Villamizar de la Universidad Central de Venezuela me propone investigar sobre los métodos de elementos finitos, en particular los relacionados con los métodos del tipo mínimos cuadrados, basándonos en el libro de Bo Nan Jiang [6]. A medida que estabamos avanzando en el estudio de dichos métodos aplicados a la ecuación de Helmholtz surgió la necesidad de incorporar las condiciones de frontera a la discretización, por lo que decidimos hacer dicha incorporación en el funcional que habitualmente se minimiza para obtener dicho método, obteniendo así una formulación del método de elementos finitos mínimos cuadrados mas general que la que conocíamos. En base a ese trabajo realice mi anterior trabajo de ascenso, haciendo una implementación en 1D y utilizando polinomios de interpolación primer grado. Luego en los años 2003-2004 dirigí un trabajo especial de grado donde se implementaba dicho método en 1D y utilizando polinomios de interpolación de grado

superior. Este trabajo fué la base para un estudio de convergencia y comparación con otros métodos (elementos finitos mixto y diferencias finitas) el cual fué publicado en el año 2006. En virtud de que el profesor Vianey Villamizar se traslado a USA a trabajar, tuve la necesidad de realizar tres pasantias de investigación en el Department of Mathematics. Brigham Young University. Provo, Utah. USA, en los años 2001, 2002 y 2004 relacionadas con este tema de investigación.

2.1 Resultados Principales del artículo [5]

En este articulo se presenta una aplicación de un método de elementos finitos mínimos cuadrados para problemas de propagación de ondas gobernadas por la ecuación de Helmholtz. Para ello se define un funcional convexo que es minimizado dando como resultado una formulación variacional que incorpora las condiciones de frontera, véase la ecuación (15). Se hace luego una generalización en aritmética de los números complejos para tener un problema variacional más general (16). Luego se hacen las sustituciones pertinentes a fin de resolver el problema en 1D. Se presenta también en la sección 4 la formulación variacional del método de Elementos Finitos Galerkin Mixto a los fines de ser comparado a posteriori con los resultados obtenidos por el método de elementos finitos mínimos cuadrados. Se presentan luego los errores y ordenes de convergencia para ambos métodos usando diversos grados de polinomios, así como una comparación de la eficiencia computacional. Las pruebas numéricas avalan un mejor comportamineto del método de elementos finitos para resolver problemas de ondas cuando el número de onda es relativamente grande en comparación con el método de elementos finitos Galerkin Mixto.

REFERENCIAS

[1] Miguel Fagúndez, Juan Medina, Carlos Cadenas y Germán Larrazabal. Mimetic Discretizations for Computacional Fluid Dynamics: One-Dimensional Case. Revista INGENIERÍA UC, Vol. 11. No. 3, 52-57 (2004).

[2] J. Castillo y R. Grone. A Matrix Analysis Approach to Higher-Order Approximations for Divergence and Gradients Satisfying a Global Conservative Law. SIAM J. Matrix Anal. Appl. 25 (1):128-142, 2003.

[3] Carlos Cadenas y Orestes Montilla. Generalización de la matriz de Vandermonde utilizada en la Construcción del Operador de Divergencia Discreta Mimética. Revista INGENIERÍA UC, Vol. 11, No. 2, 48-52(2004).

[4] Orestes Montilla, Carlos Cadenas and José Castillo. Matrix Approach to Mimetic Discretizations for Differential Operators on Non-Uniform Grids . Mathematics and Computer in Simulation, Vol. 73. No. 1-4, 215-225 (2006).

[5] Carlos Cadenas, Javier Rojas, and Vianey Villamizar. A least squares finite element method with high degree element shape functions for one-dimensional Helmholtz equation. Mathematic and Computer in Simulation , Vol. 73. No. 1-4, 76-86 (2006).

[6] Bo-Nan Jiang, The Least-Squares Finite Element Method: Theory and Applications in Computational Fluid Dynamics and Electromagnetics. Springer-Verlag, New York, 1998,

Matriz de Vandermonde generalizada para la construcción de los operadores de divergencia discreta mimética

Carlos E. Cadenas R., Orestes Montilla M.
Departamento de Matemáticas, Facultad de Ciencias y Tecnología FACYT,
Universidad de Carabobo, Valencia, Venezuela
Email: ccadenas@uc.edu.ve, omontila@uc.edu.ve

Resumen

En este trabajo se desarrolla una generalización de las entradas de las matrices de Vandermonde que son necesarias para la construcción de los operadores diferenciales discretos miméticos de orden superior, la cual cumple con un teorema análogo en espacios discretos al teorema de divergencia clásico en 1D. El resultado obtenido es aplicado a casos particulares en mallados escalonados uniformes y no uniformes.

Palabras clave: Métodos miméticos, divergencia discreta, orden superior, mallado no uniforme.

Generalized Vandermonde matrix to build the mimetic discrete divergence operators

Abstract

In this work a generalization of the inputs of Vandermonde matrices required for the construction of the discrete divergence operator of high order is developed . These operators must satisfy an analogue divergence classic theorem on discrete space in 1D. The result is applied to particular cases on uniform and non-uniform staggered grids.

Keywords: Mimetic methods, discrete divergence, high order, nonuniform grid.

1. INTRODUCCIÓN

En el modelado y/o simulación de una gran variedad de fenómenos físicos involucrados en los procesos industriales, aparecen ecuaciones diferenciales ordinarias y parciales. La mayoría de ellas pueden ser formuladas usando operadores diferenciales invariantes de primer orden, tales como, la *divergencia* y el *gradiente*. Por otro lado, es posible construir muchos esquemas de diferencias finitas en base a los operadores discretos de divergencia y gradiente, pero en la mayoría de los casos los operadores discretos clásicos no mantienen algunas propiedades físicas y matemáticas de los operadores continuos. Por ello ha surgido la necesidad de desarrollar métodos que permitan obtener los operadores que satisfagan estas propiedades; a saber, las leyes de conservación y la simetría de los operadores. También es importante que satisfagan los teoremas tradicionales del cálculo vectorial, como lo es el teorema de Green, entre otros.

En la década de los 80's fueron publicados los trabajos pioneros de Samarskii y otros [1, 2], donde se presentan los aspectos fundamentales de los métodos de *operadores de referencia*, los cuales fueron levemente modificados en la década de los 90's, donde se destacan los aportes de Castillo y otros [3, 4]. Para esta época se les denomina métodos de *operadores de soporte*.

Shashkov [5] publica un libro sobre el método de operadores de soporte. Este texto recopila toda la información existente para el momento en dicha área. A raíz de estos trabajos se ha producido un incremento importante en la investigación. Dos de las aplicaciones más relevantes aparecen en los artículos de Hyman y

Shashkov [6, 7], en donde se resuelven numéricamente ecuaciones diferenciales que modelan fenómenos electromagnéticos.

Castillo y otros [8], presentan aproximaciones en diferencias finitas conservativas de cuarto y sexto orden, tanto para la divergencia como para el gradiente en un mallado unidimensional escalonado uniforme.

Castillo y Grone [9] presentan un enfoque matricial para la generación de operadores discretos miméticos de orden superior de la divergencia y el gradiente. Aquí se desarrolla toda la metodología necesaria para generar dichos operadores basados en la discretización escalonada uniforme de un dominio unidimensional. En este mismo año, Castillo y Yasuda [10], hacen una comparación en cuanto al orden de convergencia de la aproximación numérica de un problema unidimensional, basado en dos grupos de operadores discretos de divergencia y gradiente obtenidos por la metodología dada por Castillo y Grone.

Con base en este trabajo se extiende, a mallados no uniformes, el procedimiento descrito en [9]. También se presentan las ecuaciones algebraicas necesarias para algunos casos de mallados muy específicos, como lo son los mallados uniformes y no uniformes suaves definidos por Shashkov [5].

2. ESQUEMA DE DISCRETIZACIÓN MIMÉTICA

A continuación se describe brevemente la metodología mencionada anteriormente. Primero, se construye una matriz de divergencia *S* de orden adecuado, de acuerdo al tamaño de la discretización del dominio unidimensional en el que se desea resolver la ecuación diferencial, usando las fórmulas usuales para aproximar la derivada en un punto. Dicha matriz debe satisfacer un conjunto de propiedades entre las que se pueden destacar que: S es una matriz en banda, *Centro-Skew-Simetric*, véase [11], con una estructura tipo *Toeplitz* y cumple con las propiedades de suma de los elementos de las filas iguales a cero y suma de columnas iguales a –1,0,…,0,1; estas dos propiedades se refieren al hecho de que al aplicar dicho operador a una constante debe dar como resultado cero y al teorema fundamental del cálculo, respectivamente. Como la matriz *S* construida de esta forma, usualmente no cumple con las propiedades de orden de convergencia preestablecida para el operador en todo el mallado, se procede a introducir un producto interno discreto generalizado; para así, utilizando un equivalente discreto del teorema de Green se pueda encontrar la matriz de divergencia requerida con sólo premultiplicar dicha matriz por una matriz de pesos *Q*. El problema se reduce ahora en encontrar dicha matriz *Q*, que en el mejor de los casos es una matriz diagonal positiva definida y centro-simétrica. Para ello se considera en primer lugar, la construcción de una matriz de divergencia *D*, la cual es *Centro-Skew-Simetric*. Sus filas interiores son las mismas de la matriz *S* y las filas extremas están conformadas, cada una, por dos bloques de matrices. Las filas superiores por una matriz *A* no nula y la otra nula *O* y las filas inferiores se obtienen de *A*, tal que, se mantenga la propiedad de *Centro-Skew-Simetric*. Así nuevamente, se modifica el problema a encontrar la matriz *A* que cumpla con todas las propiedades miméticas mencionadas anteriormente, más las propiedades de orden de convergencia. Para conseguir esta última matriz, en virtud de que las propiedades miméticas son lineales, se puede plantear un sistema de ecuaciones lineales $Ma = b$, donde las incógnitas ubicadas en el vector *a* son los elementos de la matriz *A*, *M* es una matriz en bloque conformada por matrices de *Vandermonde*, matrices nulas e identidades. El vector *b* es elegido, tal que, se cumplan las condiciones miméticas y de orden. Al encontrar la matriz *A* es trivial obtener la matriz de divergencia *D*. Para más detalles véase [9].

La generalización que se hará de dicha metodología consiste en conformar, para un mallado escalonado no uniforme, una matriz *M*, para lo cual es necesario encontrar nuevas matrices de *Vandermonde* que satisfagan las condiciones de orden.

La notación usada, en este artículo, para las matrices de *Vandermonde* es la clásica, dada por:

$$V(m; x_1, \cdots, x_n) = \begin{bmatrix} 1 & \cdots & 1 \\ x_1 & \cdots & x_n \\ \vdots & \ddots & \vdots \\ x_1^{\,m} & \cdots & x_n^{\,m} \end{bmatrix} \tag{1}$$

donde *m* es el orden de convergencia del operador diferencial involucrado y *n* es la cantidad de puntos utilizados en la aproximación.

3. MATRIZ DE VANDERMONDE

Para obtener las matrices de *Vandermonde* se utiliza el procedimiento clásico de desarrollar fórmulas de aproximación para derivadas en un punto. Es decir, para obtener una fórmula de aproximación para la derivada de orden *k* se construye un operador discreto en base a una combinación lineal de los valores en ciertos puntos de una función polinomial de grado *k*. Al evaluar dicha combinación lineal para polinomios de grado menor o igual a *k*, se obtiene el valor exacto de la derivada. Lo recientemente expresado no es cierto para polinomios de grado mayor a *k*.

Con base en lo anterior, sea la función de prueba $f(x) = \left(x - x_{1/2+j}\right)^n;\ \ n = 0,1,\cdots,k$; para obtener una divergencia discreta de orden *k* sobre un mallado escalonado no uniforme, donde los nodos extremos de las celdas son $x_1 < x_2 < \cdots < x_m$, con $h_i = x_{i+1} - x_i$ y sus puntos medios $x_{3/2} < x_{5/2} < \cdots < x_{m-1/2}$. Para detallar lo descrito anteriormente se presenta un ejemplo modelo, según se muestra en la Figura 1, para una configuración de cinco nodos distribuidos de manera no uniforme, teniendo así, cuatro celdas identificadas con el punto medio de las mismas.

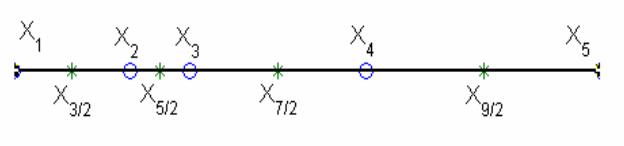

Figura 1. Mallado escalonado no uniforme.

y

$$f\left(x_{1/2+j}\right) = \sum_{i=1}^{3k/2} a_{ji} f\left(x_i\right);\quad j = 1,\cdots,k \qquad (2)$$

donde se considera sólo el caso que *k* sea par.

Para obtener la matriz de divergencia no uniforme se analizan los diferentes valores que puede tomar la variable *n* cuando la función de prueba es sustituida en la ecuación (2).

Si $n = 0$ se obtiene la ecuación homogénea:

$$\sum_{i=1}^{3k/2} a_{ji} = 0;\quad j = 1,\cdots,k \qquad (3)$$

Si $n = 1$ se obtiene:

$$\sum_{i=1}^{j} a_{ji}\left(-\sum_{m=i}^{j} h_m + \frac{h_j}{2}\right) + \sum_{i=j+1}^{3k/2} a_{ji}\left(\sum_{m=j}^{i-1} h_m - \frac{h_j}{2}\right) = 1; \qquad (4)$$

$j = 1,\cdots,k$

Si $n = 2$ se obtiene:

$$\sum_{i=1}^{j} a_{ji}\left(-\sum_{m=i}^{j} h_m + \frac{h_j}{2}\right)^2 + \sum_{i=j+1}^{3k/2} a_{ji}\left(\sum_{m=j}^{i-1} h_m - \frac{h_j}{2}\right)^2 = 0; \qquad (5)$$

$j = 1,\cdots,k$

Finalmente para toda *n* mayor que dos se tiene:

$$\sum_{i=1}^{j} a_{ji}\left(-\sum_{m=i}^{j} h_m + \frac{h_j}{2}\right)^n + \sum_{i=j+1}^{3k/2} a_{ji}\left(\sum_{m=j}^{i-1} h_m - \frac{h_j}{2}\right)^n = 0 \qquad (6)$$

$j = 1,\cdots,k$

Las ecuaciones (3)-(6) se pueden resumir en el siguiente teorema:

Teorema 1
Sea $f(x) = \left(x - x_{1/2+j}\right)^n;\ \ n = 0,1,\cdots,k$ *una función de prueba para el operador de divergencia discreto, entonces al utilizar (2) se obtiene la ecuación*

$$\sum_{i=1}^{j} a_{ji}\left(-\sum_{m=i}^{j} h_m + \frac{h_j}{2}\right)^n + \sum_{i=j+1}^{3k/2} a_{ji}\left(\sum_{m=j}^{i-1} h_m - \frac{h_j}{2}\right)^n = \delta_{1n}$$

$j = 1,\cdots,k$

que permite obtener los elementos de entrada de las matrices de Vandermonde, donde δ_{1n} *es la delta de Kronecker, definida por:*

$$\delta_{1n} = \begin{cases} 1 & \text{si } n = 1 \\ 0 & \text{si } n \neq 1 \end{cases}$$

Las entradas de las matrices de *Vandermonde* se obtienen a partir de los coeficientes de a_{ji} , que no es más que el elemento de la fila *j* y columna *i* de la matriz *A* que conforman las primeras filas del operador discreto mimético de divergencia *D*.

4. APLICACIONES

En esta sección se utilizará el Teorema 1 para obtener las entradas de las matrices de *Vandermonde*, para los casos de mallados uniformes y no uniformes suave. Para ello se considerará el intervalo [0, 1].

4.1. Mallado uniforme

En el caso del mallado uniforme $x_j = \xi_j$; $j = 1, \cdots, M$ donde $\xi_j = (j-1)/(M-1)$ representan los nodos para un espaciamiento uniforme y *M - 1* es la cantidad de celdas involucradas en la discretización. Con esta notación se calcula el tamaño del paso *h* por medio de la ecuación

$$h_j = x_{j+1} - x_j = \frac{1}{M-1} = h \tag{7}$$

aplicando el Teorema 1, se obtiene

$$\sum_{i=1}^{j} a_{ji} \left(\frac{(2i-2j-1)h}{2} \right)^n + \sum_{i=j+1}^{3k/2} a_{ji} \left(\frac{(2i-2j-1)h}{2} \right)^n = \delta_{1n}$$

$$j = 1, 2, \cdots k \tag{8}$$

Al simplificar, y haciendo las operaciones algebraicas adecuadas se llega a

$$-\sum_{i=1}^{3k/2} a_{ji} (2i - 2j - 1)^n = -\frac{2}{h} \delta_{1n} \tag{9}$$

Se multiplica por menos uno para que las ecuaciones resultantes sean las dadas en [9].

Las matrices de *Vandermonde* en este caso vienen dadas por

$$V_j = (k; 2j-1, 2j-3, \cdots, 3+2j-3k, 1+2j-3k) \tag{10}$$

$$j = 1, 2, \cdots, k$$

4.2. Mallado no uniforme suave

En esta sección se presenta el caso con mallado no uniforme, dado por $x_j = \xi_j^{\,2}$; $j = 1, \cdots, M$, donde x es una función suave que permite calcular los nodos para el espaciamiento no uniforme a partir de los nodos para un espaciamiento uniforme ξ_j descrito anteriormente. Usualmente a la discretización obtenida por medio de x_j se le denomina espacio físico y a la dada por ξ_j espacio lógico. Así

$$h_j = x_{j+1} - x_j = \frac{2j-1}{(M-1)^2} = (2j-1)h^2 \tag{11}$$

Aplicando el Teorema 1, se obtiene:

$$\sum_{i=1}^{j} a_{ji} \left(2(i-1)^2 - 2j^2 + 2j - 1 \right)^n +$$

$$\sum_{i=j+1}^{3k/2} a_{ji} \left(2(i-1)^2 - 2j^2 + 2j - 5 \right)^n = -\frac{2}{h^2} \delta_{1n} \tag{12}$$

Para que se entienda más claramente como se obtiene la matriz de *Vandermonde* a partir de esta ecuación, se ilustra considerando el orden de convergencia $k = 4$, para $j = 1$, y $n = 1$ obteniéndose

$$-a_{11} - 3a_{12} + 3a_{13} + 13a_{14} + 27a_{15} + 45a_{16} = -\frac{2}{h^2} \tag{13}$$

De los coeficientes de esta ecuación se obtienen los elementos de la matriz de *Vandermonde*,

$$V_1 = (4; -1, -3, 3, 13, 27, 45)$$

De forma similar se construyen las otras matrices de *Vandermonde* necesarias;

$$V_j = (4; x_1, x_2, \cdots, x_6) \qquad j = 1, \cdots, 4$$

A continuación se presenta la ecuación que permite obtener las matrices de *Vandermonde* para el caso general de un mallado uniforme dado por el x_j definido al inicio de esta sección

$$(-2j^2 + 2j - 1) a_{j1} + (-2j^2 + 2j + 1) a_{j2} + \cdots (-2j+1) a_{jj} +$$

$$(2j-5) a_{j(j+1)} + \cdots + \left(9\frac{k^2}{2} - 12k - 2j^2 + 2j + 3 \right) a_{j\left(\frac{3k}{2}-1\right)} +$$

$$\left(9\frac{k^2}{2} - 6k - 2j^2 + 2j - 3 \right) a_{j\left(\frac{3k}{2}\right)} = -\frac{2}{h^2} \tag{14}$$

y así la matriz de *Vandermonde* para $j = 1, 2, \cdots, k$, sería

$$V_j = (k; -2j^2 + 2j - 1, -2j^2 + 2j + 1, \cdots, -2j + 1, 2j - 5, \cdots,$$

$$9\frac{k^2}{2} - 12k - 2j^2 + 2j + 3, 9\frac{k^2}{2} - 6k - 2j^2 + 2j - 3) \tag{15}$$

5. CONCLUSIONES Y RECOMENDACIONES

En esta investigación se obtuvo una familia de funciones de prueba polinómicas, fundamentadas en las propiedades que las mismas deben cumplir para aproximar la primera derivada en un punto con un

orden de precisión preestablecido. Estas propiedades son vitales para finalmente construir el operador de divergencia discreto mimético.

De igual manera, se han presentado casos elementales de aplicación del Teorema 1, tratando de dejar claro el procedimiento usado, para que así pueda ser implementado a otros tipos de mallados no uniformes, tanto suaves como no suaves.

De una manera similar a como se construyen en este artículo las matrices de *Vandermonde* para generar el operador discreto de divergencia mimética, se pueden construir matrices de *Vandermonde* para obtener el operador discreto de gradiente mimético. Para ello se deben seleccionar otras funciones de prueba, que se adecuen a la característica de evaluar al gradiente en los puntos que representan a los nodos, los cuales denominamos también puntos enteros; de esta manera, para calcular el gradiente en dichos puntos enteros, se hace por medio de la combinación lineal de la función de prueba evaluada en los puntos que representan a las celdas, o a los que denominamos puntos medios.

Actualmente, con base en el resultado de este artículo se está desarrollando una herramienta computacional, que use cálculo simbólico e involucre el cálculo de todos los parámetros que aparecen en el producto interno generalizado que deben satisfacer los operadores de divergencia y gradiente miméticos. Estos resultados pronto serán presentados en otro artículo.

6. RECONOCIMIENTO

Esta investigación ha sido subvencionada, en parte por la partida de investigación 407 asignada a la Facultad Experimental de Ciencias y Tecnología de la Universidad de Carabobo por parte del CNU-OPSU, la cual es administrada por el Consejo de Facultad de dicha institución, así como también se utilizaron recursos provenientes de financiamiento por parte del FONACYT Carabobo.

REFERENCIAS

[1] A. Samarskii, V. Tishkin, A. Favorski, M. Shashkov, Yu. (1981). "Operational Finite Difference Schemes", Diff. Eqns., 17, 7, 854-862

[2] A. Samarskii, V. Tishkin, A. Favorski, M. Shashkov, Yu, (1982). "Employment of the Reference-Operator Method in the Construction of Finite Difference Analogs Of Tensor Operations", Diff. Eqns., 18, 7, 881-885

[3] J. Castillo, J. M. Hyman, M. Shashkov, S. Steinberg. (1995). "The Sensitivity and Accuracy of Fourth Order Finite Difference Schemes on Nonuniform Grids in one Dimension", An International Journal of Computers & Mathematics with Applications, 30, 8, 41-55

[4] J. Castillo, J. M. Hyman, M. Shashkov, S. Steinberg. (1995). "High Order Mimetic Finite Difference Methods on Nonuniform Grids", Proc. of the Third International Conference on Spectral and High Order Methods, Special Issue of Houston Journal of Mathematics, eds. A.V. Ilin and L.R. Scott Texas, USA, 347-361

[5] M. Shashkov. (1996). "Conservative Finite Difference Methods on General Grid", CRC Press, Florida, USA, pp. 359

[6] J. M. Hyman, M. Shashkov. (1998). "Mimetic Discretizations for Maxwell's Equations and Equations of Magnetic Diffusion". In J. DeSanto, ed., Math. and Numerical Aspects of Wave Propagations, (SIAM, Philadelphia, 1998) 561--563, Proc. of the Fourth International Conference on Mathematical and Numerical Aspects of Wave Propagation, Golden, Colorado, June 1-5

[7] J.M. Hyman, M. Shashkov. (2001). "Mimetic Finite Difference Methods for Maxwell's Equations and the Equations of Magnetic Diffusion". Progress in Electromagnetics Research, PIER 32, 89-121

[8] J.E. Castillo, J.M. Hyman, M. Shashkov, S. Steinberg. (2001). "Fourth and Sixth-Order Conservative Finite Difference Approximations of the Divergence and Gradient". Appl. Num. Math., 37, 171-187.

[9] J. E. Castillo and R. D. Grone. (2003). "A Matrix Analysis Approach to Higher-Order Approximations for Divergence and Gradients Satisfying a Global Conservation Law", SIAM J. Matrix Anal. Appl. 25, 1, 128-142

[10] J. E. Castillo, M. Yasuda. (2003). "Comparison of two matrix operator formulations for mimetic divergence and gradient discretizations", Computational Science Research Center. San Diego State University

[11] A. L. Andrew. (1998). "Centrosymmetric matrices". SIAM Rev., 40, 697-699.

Discretizaciones miméticas para dinámica de fluidos computacional: Caso uni-dimensional

M. Fagúndez[(1)], J. Medina[(1)], C. Cadenas[(2)], G. Larrazabal[(1)]
[(1)]*Departamento de Computación, FACYT-Universidad de Carabobo, Valencia, Venezuela*
[(2)] *Departamento de Matemática, FACYT- Universidad de Carabobo, Valencia, Venezuela*
Email: miguelomar@cantv.net;juanruben@cantv.net;ccadenas@uc.edu.ve;glarraza@uc.edu.ve

Resumen

Se presentan resultados preliminares en la simulación de flujo de fluidos uni-dimensional con métodos conservativos. Se exhiben diferentes esquemas numéricos para resolver las ecuaciones de Navier-Stokes y de compresibilidad artificial, dos de ellos son explícitos y los restantes implícitos. El primer esquema usa el método de operadores de soporte, el segundo mezcla este método con el de Crank-Nicolson, y los otros usan el método de Castillo Grone 2-2-2. Para resolver los sistemas de ecuaciones obtenidos por medio de los métodos implícitos, se usa la librería UCSparseLib la cual ha sido desarrollada en ANSI C. Además, se desarrolló un conjunto de herramientas para mostrar los resultados gráficamente usando OpenGL.

Palabras clave: Métodos miméticos, Navier-Stokes, dinámica de fluidos.

Mimetic discretizations for computational fluid dynamics: uni-dimensional case

Abstract

Preliminary results in uni-dimensional fluid flow simulation based on conservative methods are presented. Several numerical schemes to solve Navier-Stokes and artificial compressibility equations, two of them explicit and two implicit are exhibited. The first uses Support-Operators method, the second scheme mixes this method with Crank-Nicholson's and the others uses 2-2-2 Castillo-Grone method. For solving the systems of linear equations obtained through implicit methods, the UCSparseLib library is used which has been developed on ANSI C. Furthermore, a set of tools was developed to display results graphically using OpenGL.

Keywords: Mimetic methods, Navier-Stokes, fluid dynamics

1. INTRODUCTION

The mimetic methods are based on the construction of discrete differential operators that mimic some fundamental properties of divergence and gradient operators, among others. About two decades ago the Support-Operators method was developed [4,5], which is based on considering discrete analog of Green's Theorem to obtain a derived discrete operator starting from a prime discrete operator, i. e., a differential operator is imposed as the prime, and starting from the discrete Green's identity the derived operator is obtained. For furthers details on this methodology see [1]. For several methods related to the construction of mimetic discrete operators [6,7,9,10], as well as some of their applications [8,11], check http://cnls.lanl.gov/~shashkov. A methodology to build discrete operators satisfaying Green´s generalized discrete theorem has been recently developed in [2], where higher order mimetic differential operatos can be built in the inner nodes as in the boundaries for 1D uniform grid. In this work, a set of operators obtained by the Support-Operators method as well as Castillo-Grone methods is used in order to simulate the flow of fluids in one dimension. In all cases staggered grids were used being necessary the using of grid functions. Some basic topics allowing the understadins of the notation to be used in the next sections are now present.

2. PRELIMINARY

In this section the equations the equations governing the behavior of the fluids flow to be simulated are presented, as well as an introduction to the staggered uniform grids and grid functions generation. The discrete operators to obtain the differences schemes are also presented.

2.1. Model problem

Next, the equations to use in the One-dimensional flow of fluid simulations are show. They are the Navier-Stokes and Artificial Compressibility equations

$$\frac{\partial V}{\partial t}+V\frac{\partial V}{\partial x}=-\frac{1}{\rho}\frac{\partial p}{\partial x}+\nu\frac{\partial^2 V}{\partial x^2} \quad \text{on } (a,b) \text{ and } 0<t<\infty \qquad (1)$$

$$\frac{1}{\beta}\frac{\partial p}{\partial t}+\frac{\partial V}{\partial x}=0 \quad \text{on } (a,b) \text{ and } 0<t<\infty \qquad (2)$$

where p is the pressure, V the velocity, ρ the density, ν the viscosity, t is the time and β the artificial compressibility parameter. Test cases were built using Dirichlet boundary conditions.

2.2. Staggered grid and grid functions

In this work a staggered uniform grid is used, which is defined by M nodes along the one dimension domain considered and M-1 cells. A cell is given by the set of points in between any pair of consecutive nodes. Usually, in order to identify a cell any point inside of it is utilized. For this porpuse, in this work is used as its identification. Hence, it there is a set of nodes $\{x_1, x_2, \cdots, x_i, x_{i+1}, \cdots, x_{M-1}, x_M\}$ with x_1=0 and $x_M = 1$, then the set of cells will be denoted as $\{x_{3/2}, x_{5/2}, \cdots, x_{i-1/2}, x_{i+1/2}, \cdots, x_{M-3/2}, x_{M-1/2}\}$ where $x_{i+1/2} = (x_{i+1} + x_i/2); i = 1, \cdots, M-1$

As usually, two classes of grid functions are used: a nodal-valued and a cell-valued. The nodal-valued functions are defined as $f: HC \rightarrow HN$ whereas the cell-valued ones as of the form $g: HN \rightarrow HC$ such that HC is the space for cell-valued grid functions and HN, the space for nodal discretization. Figure 1 shows the staggered grid and grid functions to be used. The

size of the cell will be denoted by:

$$h = x_{i+1} - x_i; i = 1, \cdots, M-1$$

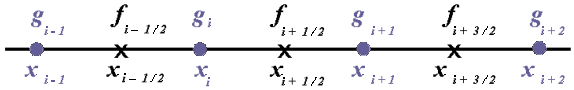

Figure 1. The staggered grid and grid functions.

2.3. Discrete operators

The discrete divergence and gradient operators given by the Support-Operators method for a staggered uniform grid are:

$$(\mathrm{D}g)_{i+\frac{1}{2}} = \frac{g_{i+1}-g_i}{h}, \quad 1 \le i \le M-1 \qquad (3)$$

$$(\mathrm{G}f)_i = \begin{cases} \dfrac{f_{3/2}-f_1}{h/2}, & i=1 \\ \dfrac{f_{i+1/2}-f_{i-1/2}}{h}, & 2 \le i \le M-1 \\ \dfrac{f_M - f_{M-1/2}}{h/2}, & i=M \end{cases} \qquad (4)$$

In the 2-2-2 Castillo-Grone method, the equations for the gradient operator on the boundaries are modified, being obtained:

$$(\mathrm{G}f)_1 = \begin{cases} \dfrac{-\frac{4}{3}f_1+\frac{3}{2}f_{3/2}-\frac{1}{6}f_{5/2}}{h/2}, & i=1 \\ \dfrac{\frac{4}{3}f_M-\frac{3}{2}f_{M-1/2}+\frac{1}{6}f_{M-3/2}}{h/2}, & i=M \end{cases} \qquad (5)$$

3. EXPLICIT METHODS

Two explicit difference equations for the problem given in (1) and (2) are here presented, using the discrete operators introduced in the previous section. In all the cases the differential equation is evaluated on a generic point x_i or $x_{i+1/2}$. The cell-valued functions are approximated by the average of the functions evaluated on the nodes. This is a second order approximation:

$$f_{i+1/2} = \frac{f_{i+1} + f_i}{2} + O(h^2) \tag{6}$$

Since equations (1) and (2) hold for every point of the domain, this is particularly true on the cells of the grid when time $t = n\Delta t$, where Δt is the size of the discretization of the time and $n = 0, 1, 2,\ldots$ This is

$$\frac{\partial V^n_{i+1/2}}{\partial t} + V^n_{i+1/2}\frac{\partial V^n_{i+1/2}}{\partial x} = -\frac{1}{\rho}\frac{\partial p^n_{i+1/2}}{\partial x} + \nu\frac{\partial^2 V^n_{i+1/2}}{\partial x^2} \tag{7}$$

$$\frac{1}{\beta}\frac{\partial p^n_{i+1/2}}{\partial t} + \frac{\partial V^n_{i+1/2}}{\partial x} = 0 \tag{8}$$

Now, equation (6) is used to approximate the discrete gradient operator of the pressure, i.e. $\partial p^n_{i+1/2} \big/ \partial x$

Then, approximations (3), (4) and (5) are applied to the operators involved in (7) and (8). On inner points, this is

$$V^{n+1}_{i+1/2} = V^n_{i+1/2}\left(1 - r\delta_1 V^n\right) - \frac{r}{\rho}\delta_1 p^n + s\delta_2 V^n$$

$$p^{n+1}_{i+1/2} = p^n_{i+1/2} - q\delta_1 V^n$$

Where $r = \Delta t/2h$, $s = \Delta t\nu/h^2$, $q = \beta\Delta t\nu/2h$ with $h = x_{i+1} - x_i$ and the difference operators in δ_1 and δ_2 are defined by

$$\delta_1 W^n = W^n_{i+3/2} - W^n_{i-1/2}$$

and

$$\delta_2 W^n = W^n_{i+3/2} - 2W^n_{i+1/2} + W^n_{i-1/2}$$

It is important to say that both δ_1 and δ_2 are used in the Support-Operators and Castillo-Grone methods. The difference between those methods is the gradient operator approximation on the boundaries.

Next, the equations for the left boundary are

$$V^{n+1}_{3/2} = V^n_{3/2}\left(1 - r\delta_5 V^n\right) - \frac{r}{\rho}\delta_3 p^n + s\delta_4 V^n$$

and

$$p^{n+1}_{3/2} = p^n_{3/2} - q\delta_5 V^n$$

where $\delta_5 W^n = W^n_{5/2} + W^n_{3/2} - 2W^n_1$ and δ_3 and δ_4 depend on the method used.

$$\delta_3 W^n = W^n_{5/2} + W^n_{3/2} - 2W^n_1$$

and

$$\delta_4 W^n = W^n_{5/2} - 3W^n_{3/2} + 2W^n_1$$

for the Support-Operators method and

$$\delta_3 W^n = -(8/3)W^n_1 + 2W^n_{3/2} + (2/3)W^n_{5/2}$$

and

$$\delta_4 W^n = (4/3)W^n_{5/2} - 4W^n_{3/2} + (8/3)W^n_1$$

for the Castillo-Grone method.

For the right boundary they are

$$V^{n+1}_{N-1/2} = V^n_{N-1/2}\left(1 - r\delta_8 V^n\right) - \frac{r}{\rho}\delta_6 p^n + s\delta_7 V^n$$

and

$$p^{n+1}_{N-1/2} = p^n_{N-1/2} - q\delta_8 V^n$$

where $\delta_8 W^n = 2W^n_N - W^n_{N-1/2} - W^n_{N-3/2}$ and δ_6 and δ_7 depend on the method used.

$$\delta_6 W^n = 2W^n_N - W^n_{N-1/2} - W^n_{N-3/2}$$

and

$$\delta_7 W^n = 2W^n_N - 3W^n_{N-1/2} + W^n_{N-3/2}$$

for the Support-Operators method and

$$\delta_6 W^p = (8/3)W^p_N - 2W^p_{N-1/2} - (2/3)W^p_{N-3/2}$$

and

$$\delta_7 W^p = (8/3)W^p_N - 4W^p_{N-1/2} + (4/3)W^p_{N-3/2}$$

for the Castillo-Grone method.

4. IMPLICIT METHODS

In this section the difference equations are presented in an implicit way for the problem given in (1) and (2) using the Cranck-Nicolson method and the discrete operators given in the previous section.

Substituting the difference operators (3-6), into equations (1) and (2) it is obtained:

$$V_{i+1/2}^{n+1} + V_{i+1/2}^{n} \frac{r}{2}\delta_1 V^{n+1} + \frac{r}{2\rho}\delta_1 p^{n+1} - \frac{s}{2}\delta_2 V^{n+1} =$$

$$V_{i+1/2}^{n}\left(1 - \frac{r}{2}\delta_1 V^{n}\right) - \frac{r}{2\rho}\delta_1 p^{n} + \frac{s}{2}\delta_2 V^{n}$$

$$p_{i+1/2}^{n+1} + \frac{q}{2}\delta_1 V^{n+1} = p_{i+1/2}^{n} - \frac{q}{2}\delta_1 V^{n}$$

Next, the equations for the left boundary are

$$V_{3/2}^{n+1} + V_{3/2}^{n} \frac{r}{2}\delta_5 V^{n+1} + \frac{r}{2\rho}\delta_3 p^{n+1} - \frac{s}{2}\delta_4 V^{n+1} =$$

$$V_{3/2}^{n}\left(1 - \frac{r}{2}\delta_5 V^{n}\right) - \frac{r}{2\rho}\delta_3 p^{n} + \frac{s}{2}\delta_4 V^{n}$$

$$p_{3/2}^{n+1} + \frac{q}{2}\delta_5 V^{n+1} = p_{3/2}^{n} - \frac{q}{2}\delta_5 V^{n}$$

And for the right boundary they are

$$V_{N-1/2}^{n+1} + V_{N-1/2}^{n} \frac{r}{2}\delta_8 V^{n+1} + \frac{r}{2\rho}\delta_6 p^{n+1} - \frac{s}{2}\delta_7 V^{n+1} =$$

$$V_{N-1/2}^{n}\left(1 - \frac{r}{2}\delta_8 V^{n}\right) - \frac{r}{2\rho}\delta_6 p^{n} + \frac{s}{2}\delta_7 V^{n}$$

$$p_{N-1/2}^{n+1} + \frac{q}{2}\delta_8 V^{n+1} = p_{N-1/2}^{n} - \frac{q}{2}\delta_8 V^{n}$$

5. NUMERICAL TESTS

The purpose of these tests is to verify the behavior of the presented schemes. See the matrix structure for implicit cases in the Figure 2. To guarantee the stability of the method is used $\beta = \nu\Delta t/\Delta x^2$. For explicit methods $\Delta t = 10^{-5}$ and for implicit methods $\Delta t = 10^{-3}$ with an initial value $\Delta x^0 = 10^{-2}$. This value is decreased using $\Delta x^{i+1} = \Delta x^i/2$, $i = 0,1,2,...$

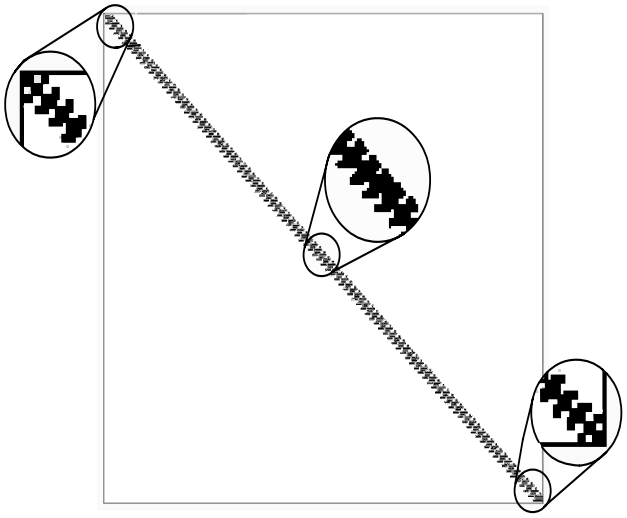

Figure 2. Sparse matrix structure for implicit methods.

5.1. Case 1

A laminar flow, incompressible with constant cinematic viscosity between two parallel walls separated by a distance H is considered. Initially the two walls and the fluid are in stationary state. In the instant $t = 0$, one of the walls moves at a constant speed V_0. This problem has an exact solution given by

$$V / V_0 = 1 - x / H - 2\sum_{n=1}^{\infty} \frac{1}{n\pi} sen(n\pi x / H)\exp(-n^2\pi^2 \nu t / H^2)$$

Once all simulations have been made, it is possible to obtain the behavior shown in Figure 3, in which the value of the speed can be observed for each one of the nodes in a given moment.

To stop the iterations it is used a tolerance of 10^{-2} for the energy norm of the error given by:

$$\left\| u^h \right\| = \left(\sum_{i=1}^{M-1} \left(u_i^h\right)^2 * \left(x_{i+1} - x_i\right) \right)^{1/2}$$

.

Figures 4 and 5 show the results obtained using the explicit and implicit methods respectively.

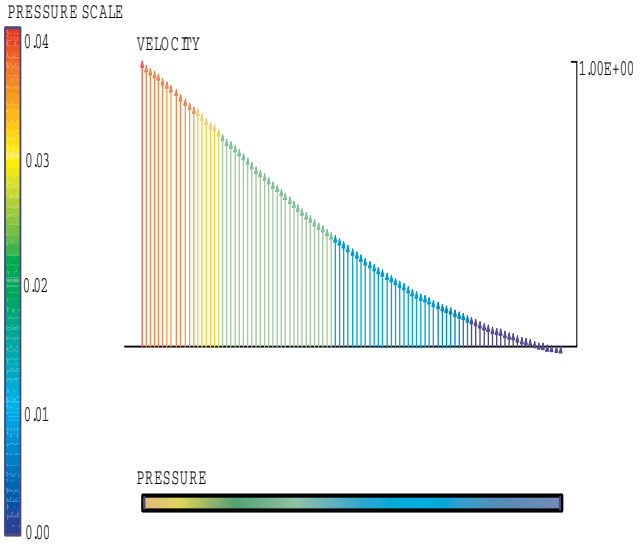

Figure 3. Simulation with the explicit Support-Operators method. $\rho = 996$, $\nu = 0.804$, $\Delta t = 10^{-5}$ and $\Delta t = 10^{-2}$.

5.2. Case 2

The same as in the previous test, a fluid is considered between two parallel walls, but in this case the walls are fixed. An initial constant speed is set for all the nodes on the grid in the time t=0, as well as a constant pressure bigger than zero. The simulation process generates a parabolic function in the speed profile, which diminish while the time in the simulation increases. See Figure 6.

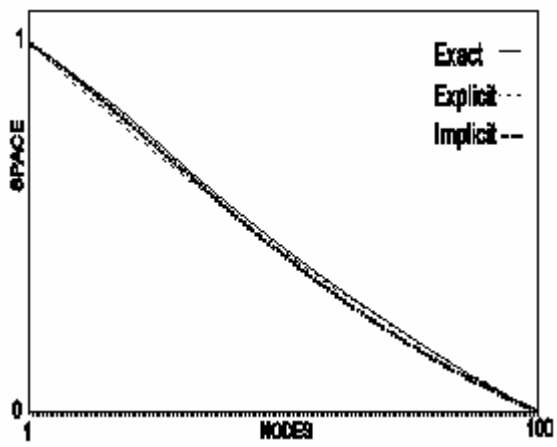

Figure. 4. Comparison of Support-Operators Explicit and Implicit results with the exact solution.

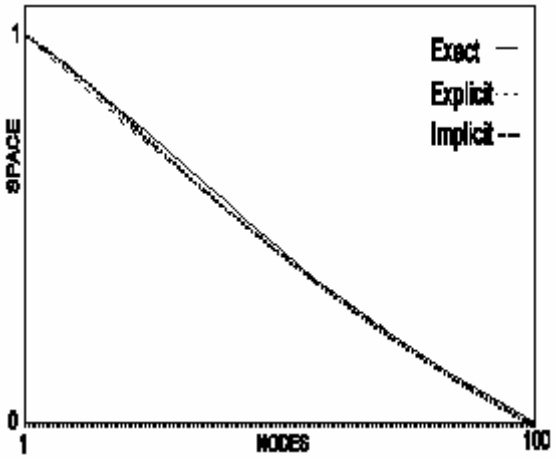

Figure 5. Comparison of Castillo-Grone 2-2-2 Explicit and Implicit results with the exact solutions.

5.3. Case 3

In this case, constant speeds are set for each wall, but in opposite sense. The behavior of the simulation tends to a straight line along the profile of speeds of each one of the walls. See Figure 7.

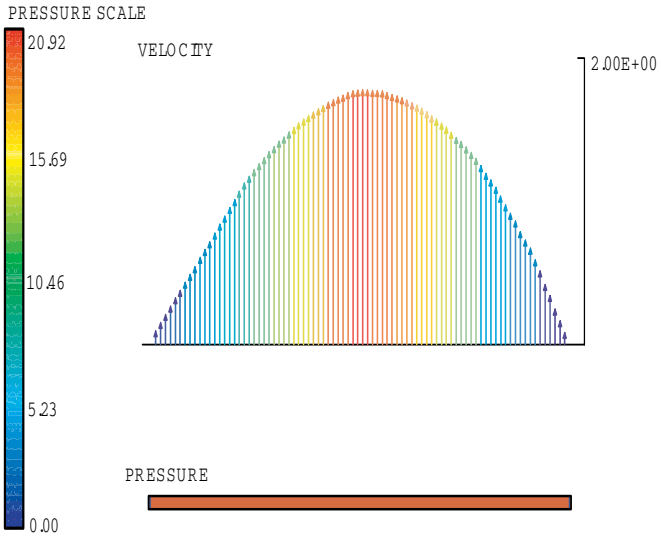

Figure 6. Case 2: Implicit Support-Operators method. $\rho = 996$, $\nu = 0.804$, $\Delta t = 10^{-3}$ and $\Delta t = 10^{-2}$.

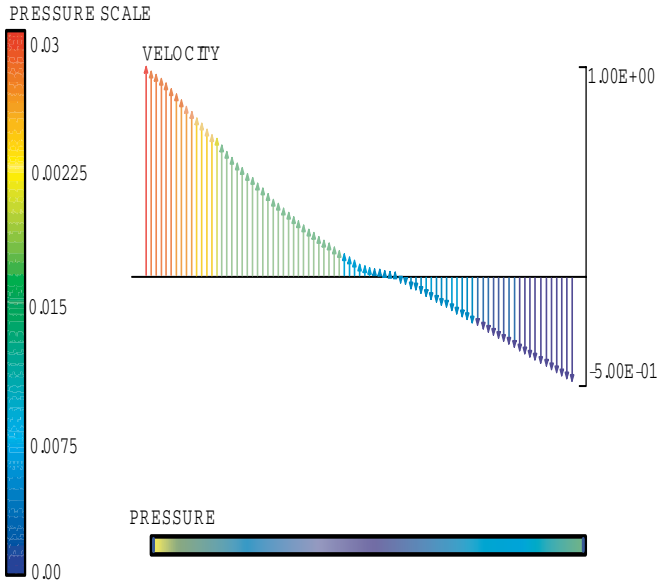

Figure 7. Case 3: Implicit Castillo-Grone 2-2-2 method. $\rho = 996$, $\nu = 0.804$, $\Delta t = 10^{-3}$ and $\Delta x = 10^{-2}$.

6. CONCLUSIONS

- The implemented methods converge in all test cases.
- The results obtained in the simulations, in function of the boundary conditions, present a similar behavior to that which happens in reality.
- In all cases, the tolerance of the error in the calculation of the solution of the linear systems by the BicGSTAB and GMRES methods were 10^{-12}, accuracy generally reached in the initial iterations. That is why it is considered that it is not necessary to change the method unless higher precision is required.
- In the calculation of the approximations of the differential equations through the mimetic methods, the error of the energy norm with regard to an analytic solution, is in the order of 10^{-2}, being better with the approximation formulated by the 2-2-2 methods.

7. ACKNOWLEDGMENTS

To Professor José Castillo of San Diego State University for his collaboration.

REFERENCES

[1] M. Shashkov. Conservative Finite-Difference Methods on General Grids. CRC Press. Florida, USA, 1996

[2] J. Castillo and R. Grone A Matrix Analysis Approach to Higher-Order Approximations for Divergence and Gradients Satisfying a Global Conservation Law. SIAM J. Matrix Anal. Appl. 25(1):128-142, 2003.

[3] G. Larrazabal. UCSparseLib: Una Librería Numérica para la Resolución de Sistemas Lineales Dispersos. Facultad Experimental de Ciencias y Tecnología, Departamento de Computación, Universidad de Carabobo, 2002.

[4] Samarskii, A., Tishkin, V., Favorskii, A., Shashkov, M. Operational Finite-Difference Schemes, Diff. Eqns., 17(7):854-862, 1981.

[5] Samarskii, A., Tishkin, V., Favorskii, A., Shashkov, M. Employment of the Reference-Operator Method in the Constrution of Finite Difference Analog of Tensor Operations, Diff. Eqns., 18(7):881-885, 1982.

[6] J.E. Castillo, J. M. Hyman, M.J. Shashkov and S. Steinberg, High-Order Mimetic Finite Difference Methods on Nonuniform Grids, In ICOSAHOM-95, Proc. of the Third International Conference on Spectral and High Order Methods. Houston. Texas, 5-9. June, 1995.Special Issue of Houston Journal of Mathematics

[7] J.E. Castillo, J.M. Hyman, M. Shashkov and S. Steinberg, Fourth-and Six-Order Conservative Finite Difference Approximations of the Divergence and Gradient, Applied Numerical Mathematics, 37:171-187. 2001.

[8] J. Hyman, M. Shashkov and Stanly Steinberg, The Numerical Solution of Diffusion Problems in Strongly Heterogeneous Non-Isotropic Materials, Journal of Computational Physics 132:130-148. 1997.

[9] J. Hyman and M. Shashkov, Adjoint Operators for the Natural Discretizations of the Divergence, Gradient, and Curl on Logically Rectangular Grids, Applied Numerical Mathematics 25:413-442. 1997.

[10] J. Hyman, M. Shashkov, Approximation of Boundary Conditions for Mimetic Finite-Difference Methods, Computers Math. Applic. 36(5):79-99. 1998.

[11] M. Shashkov and S. Steinberg, Solving Diffusion Equations with Rough Coefficients in Rough Grids, Journal of Computational Physics. 129:383-405. 1996.

[12] M. Potter, D. Wiggert, Mecánica de Fluidos, Thompson. 2002.

Available online at www.sciencedirect.com
ScienceDirect
Mathematics and Computers in Simulation 73 (2006) 76–86
MATHEMATICS AND COMPUTERS IN SIMULATION
www.elsevier.com/locate/matcom

A least squares finite element method with high degree element shape functions for one-dimensional Helmholtz equation

Carlos E. Cadenas[a,*], Javier J. Rojas[b], Vianey Villamizar[c]

[a] *Dpto. de Matemáticas, FACYT, Universidad de Carabobo, Valencia, Venezuela*
[b] *Dpto. de Computación, FACYT, Universidad de Carabobo, Valencia, Venezuela*
[c] *Department of Mathematics, BYU, Provo, UT 84602, USA*

Available online 27 July 2006

Abstract

An application of least squares finite element method (LSFEM) to wave scattering problems governed by the one-dimensional Helmholtz equation is presented. Boundary conditions are included in the variational formulation following Cadenas and Villamizar's previous paper in Cadenas and Villamizar [C. Cadenas, V. Villamizar, Comparison of least squares FEM, mixed galerkin FEM and an implicit FDM applied to acoustic scattering, Appl. Numer. Anal. Comput. Math. 1 (2004) 128–139]. Basis functions consisting of high degree Lagrangian element shape functions are employed. By increasing the degree of the element shape functions, numerical solutions for high frequency problems can be easily obtained at low computational cost. Computational results show that the order of convergence agrees with well known a priori error estimates. The results compare favorably with those obtained from the application of a mixed Galerkin finite element method (MGFEM).

Keywords: Least squares finite element method; Galerkin mixed finite element method; Convergence rate; Helmholtz equation; Wave scattering

1. Introduction

An important class of Sturm–Liouville boundary value problems is wave scattering phenomena modelled by the Helmholtz equation. The numerical solution of these scattering problems has been an area of intensive research activity for more than four decades, and there have been several different approaches. One of them is the boundary integral equations method. It is based on an equivalent integral equations formulation of the boundary value problem, originally given in terms of partial differential equations. One of the earliest papers [2], in which these integral equations were discretized and numerically solved appeared in 1963 and treated acoustic wave scattering. A generalization of this technique has become known as the boundary element method. A good description of the theory and applications is contained in [12]. Finite difference time domain methods have also become an important numerical technique in wave scattering, especially for electromagnetic waves [11,9]. A comprehensive review of the development and applications of this method can be found in [10]. Finite element techniques represent an alternative approach to the numerical solution of wave problems modelled by the Helmholtz equation. One of the first papers using this technique was written by Aziz and Werschulz [1]. This approach has emphasized the application of the classical Galerkin finite element method.

* Corresponding author.
E-mail addresses: ccadenas@uc.edu.ve (C.E. Cadenas), jrojas@uc.edu.ve (J.J. Rojas), vianey@math.byu.edu (V. Villamizar).

0378-4754/$32.00 © 2006 IMACS. Published by Elsevier B.V. All rights reserved.
doi:10.1016/j.matcom.2006.06.013

A detailed account of the classical Galerkin finite element method applied to the Helmholtz equation can be found in [5]. The difficulty in obtaining good approximations for wave scattering problems modelled by the Helmholtz equation resides in the frequency values k. High frequencies may cause an excessive number of nodes and, as a consequence, prohibitively high computational time for any numerical method.

In recent years, an alternative finite element approach based on a different variational formulation has been used. This variational formulation is obtained by minimizing the least squares errors. But, instead of applying the error minimization on the second order Helmholtz equation, it is applied on an equivalent first order system. This technique is known as the least squares finite element method (LSFEM). An excellent review is found in [6]. Application of LSFEM to boundary value problems (BVP) modelled by Sturm–Liouville-type equations in one dimension first appeared in [4]. In this work, LSFEM was applied to three model problems with homogeneous boundary conditions. The results obtained were compared with those obtained from the application of the mixed Galerkin finite element method (MGFEM) to the same problems. These numerical tests indicated better convergence rates for LSFEM. In fact, optimal rates in both primary and secondary variables were obtained by the use of LSFEM. However, in [3] it was found that LSFEM applied to the Helmholtz equation compared unfavorably with MGFEM for relatively high frequencies. Computational experiments revealed that application of LSFEM, using piecewise linear basis for moderately high frequencies, as for example $k = 30$, required an enormous number of elements. Therefore, the amount of computation, and, as consequence, the CPU time employed by LSFEM was much greater than the time used by MGFEM to solve the problem for the same frequency. Here, we will show that increasing the degree of the element shape functions, in the range $D = 2$–5, allows approximation of the primary and secondary variables at low computational cost using LSFEM, even for relatively high frequencies.

Consider the following boundary value problem (BVP) given by the linear second order ordinary differential equation:

$$f_1(x)u''(x) + f_2(x)u'(x) + f_3(x)u(x) = f_4(x), \qquad x \in \Omega = (a, b) \subset \mathbb{R}, \tag{1}$$

subject to the boundary conditions:

$$\varepsilon_1 u'(a) + \varepsilon_2 u(a) = \varepsilon_3, \tag{2}$$

$$\varsigma_1 u'(b) + \varsigma_2 u(b) = \varsigma_3. \tag{3}$$

It is assumed that Eq. (1) is a regular Sturm–Liouville-type equation where f_1, f_2 and f_3 are real-valued and continuous functions defined on the domain Ω, $f_1 > 0$, $f_1' = f_2$, the functions f_4 and u are complex-valued functions, and ε_j, ς_j are complex constants for $j = 1, 2$ and 3. It is also assumed that $\lambda = 0$ is not an eigenvalue of the related Sturm–Liouville eigenvalue problem, so that the BVP has a unique solution [7].

In [3], Cadenas and Villamizar used global piecewise linear approximation functions to obtain the least squares finite element approximation for the solution of a scattering problem modelled by the one-dimensional Helmholtz equation. Here, we are interested in the application of LSFEM to approximate the solution of the more general BVP (1)–(3) using piecewise Lagrange interpolating polynomials of higher degree as basis functions. All finite element calculations are carried out locally for each of the elements. As usual, the approximate solution to Eq. (1) is obtained by solving an algebraic linear system of equations that is defined by a hermitian matrix. Additionally, for comparison purposes, a mixed Galerkin finite element method with piecewise high degree Lagrange polynomials as basis functions is used. In either case, Eq. (1) must be transformed into an equivalent first order linear system of ordinary differential equations. The BVP (1)–(3) can be easily reduced to a first order linear system of ODE's by introducing the new dependent variable $w = u'$. In fact, it can be rewritten as

$$w - u' = 0, \tag{4}$$

$$f_1 w' + f_2 w + f_3 u = f_4, \tag{5}$$

$$\varepsilon_1 w(a) + \varepsilon_2 u(a) = \varepsilon_3, \tag{6}$$

$$\varsigma_1 w(b) + \varsigma_2 u(b) = \varsigma_3. \tag{7}$$

An outline of the paper is as follows. In Section 2, we present the LSFEM variational formulation of the BVP governed by the linear system of first order ODE's (4) and (5) with boundary conditions (6) and (7). Then, in Section 3, the variational formulation of the mixed Galerkin finite element method corresponding to the same BVP is described.

Next, in Section 4, the algebraic linear systems obtained from the variational formulations of the two finite element methods considered in this paper are given. Then, in Section 5, some numerical tests upon a special case of the BVP (1)–(3) are performed. More precisely, both finite element methods are applied to obtain approximate solutions of a one-dimensional acoustic scattering problem. This problem was defined in [3] as

$$p''_{\mathrm{sc}}(x) + k^2 p_{\mathrm{sc}}(x) = 0, \quad 0 < x < 1, \tag{8}$$

$$p'_{\mathrm{sc}}(0) = \mathrm{i}k, \tag{9}$$

$$\frac{\mathrm{d}p_{\mathrm{sc}}}{\mathrm{d}x}(1) - \mathrm{i}kp_{\mathrm{sc}}(1) = 0, \tag{10}$$

where $p_{\mathrm{sc}}(x)$ is the scattered pressure and k is referred to as the wavenumber. Eq. (10) is the well-known Sommerfeld radiation condition which is usually applied at infinity for unbounded domains. Nevertheless, for one-dimensional problems like this one, the Sommerfeld radiation condition is exactly satisfied anywhere on the x-axis. Thus, the domain of the BVP may be confined to a finite interval. The exact solution of the boundary value problem (8)–(10) is the stationary wave given by $p_{\mathrm{sc}}(x) = \mathrm{e}^{\mathrm{i}kx}$. We compare the performance of the two finite element methods by studying the order of convergence for each one of them for different values of the wavenumber k, ranging from 1 to 90. Finally, in Section 6, we make some conclusions about the numerical results obtained from the various tests performed in Section 5.

2. Formulation of the LSFEM

The BVP (4)–(7) can be written in a more general form as

$$\mathbf{Au} = \mathbf{f}, \qquad x \in \Omega = (a, b) \subset \mathbb{R}, \qquad \mathbf{B}_1\mathbf{u}(a) = g_1, \qquad \mathbf{B}_2\mathbf{u}(b) = g_2, \tag{11}$$

where $\mathbf{A}$ is a linear first order differential operator defined as

$$\mathbf{A} = \mathbf{A}_1\frac{\mathrm{d}}{\mathrm{d}x} + \mathbf{A}_0 = \begin{bmatrix} 0 & -1 \\ f_1 & 0 \end{bmatrix}\frac{\mathrm{d}}{\mathrm{d}x} + \begin{bmatrix} 1 & 0 \\ f_2 & f_3 \end{bmatrix}. \tag{12}$$

The symbols $\mathbf{u}$ and $\mathbf{f}$ represent complex vector functions defined as $\mathbf{u} = [\, w \; u \,]^{\mathrm{T}}$, and $\mathbf{f} = [\, 0 \;\; f_4 \,]^{\mathrm{T}}$, respectively. The boundary conditions are defined through the linear algebraic operators $\mathbf{B}_1 = [\, \varepsilon_1 \;\; \varepsilon_2 \,]$ and $\mathbf{B}_2 = [\, \varsigma_1 \;\; \varsigma_2 \,]$. The right-hand sides of these boundary conditions, $g_1 = \varepsilon_3$ and $g_2 = \varsigma_3$, are complex constants. We define a set V as an appropriate subspace of $\mathbf{L}_2(\Omega)$ (product space) such that A maps the subspace V into $\mathbf{L}_2(\Omega)$. The function $\mathbf{f}$ is a complex-valued vector function that belongs to the product space $\mathbf{L}_2(\Omega)$. The LSFEM analyzed in this work is similar to the one studied in [6], but it includes the boundary conditions in the variational formulation. In fact, it consists of finding a function $\mathbf{u} \in V$, such that $\mathbf{u}$ minimizes the quadratic functional:

$$I(\mathbf{u}) = \frac{1}{2}\|\mathbf{Au} - \mathbf{f}\|^2 + \frac{1}{2}|\mathbf{B}_1\mathbf{u} - g_1|_a^2 + \frac{1}{2}|\mathbf{B}_2\mathbf{u} - g_2|_b^2 = \frac{1}{2}(\mathbf{Au} - \mathbf{f}, \mathbf{Au} - \mathbf{f}) + \frac{1}{2}\overline{(\mathbf{B}_1\mathbf{u}(a) - g_1)}(\mathbf{B}_1\mathbf{u}(a) - g_1)$$
$$+ \frac{1}{2}\overline{(\mathbf{B}_2\mathbf{u}(b) - g_2)}(\mathbf{B}_2\mathbf{u}(b) - g_2).$$

The line segment over some of the terms in the previous equation is used to designate the complex conjugate of the expression under it. A necessary condition for the existence of the function $\mathbf{u} \in V$ is that the first variation of the functional $I(\mathbf{u})$ vanishes for all admissible vector functions $\mathbf{v} = [\, v_1 \;\; v_2 \,]^{\mathrm{T}} \in V$, i.e.:

$$\lim_{t\to 0}\frac{\mathrm{d}I}{\mathrm{d}t}(\mathbf{u} + t\mathbf{v}) = 0. \tag{13}$$

It is easy to prove that (13) is equivalent to

$$\frac{1}{2}((\mathbf{Au} - \mathbf{f}, \mathbf{Av}) + (\mathbf{Av}, \mathbf{Au} - \mathbf{f}) + \overline{(\mathbf{B}_1\mathbf{u}(a) - g_1)}\mathbf{B}_1\mathbf{v}(a) + \overline{\mathbf{B}_1\mathbf{v}(a)}(\mathbf{B}_1\mathbf{u}(a) - g_1)$$
$$+ \overline{(\mathbf{B}_2\mathbf{u}(b) - g_2)}\mathbf{B}_2\mathbf{v}(b) + \overline{\mathbf{B}_2\mathbf{v}(b)}(\mathbf{B}_2\mathbf{u}(b) - g_2)) = 0. \tag{14}$$

Using complex numbers algebraic properties and the definition of the inner product in $\mathbf{L}_2(\Omega)$ for complex-valued vector functions, Eq. (14) leads to the variational formulation of the LSFEM. This is, find $\mathbf{u} \in V$ such that

$$Re(\mathbf{Au} - \mathbf{f}, \mathbf{Av}) + Re(\overline{\mathbf{B}_1\mathbf{v}(a)}(\mathbf{B}_1\mathbf{u}(a) - g_1)) + Re(\overline{\mathbf{B}_2\mathbf{v}(b)}(\mathbf{B}_2\mathbf{u}(b) - g_2)) = 0 \tag{15}$$

for all admissible functions $\mathbf{v} \in V$. Instead of solving (15), we obtain approximate solutions for the more general variational problem: Find $\mathbf{u} \in V$ such that

$$(\mathbf{Au} - \mathbf{f}, \mathbf{Av}) + \overline{\mathbf{B}_1\mathbf{v}(a)}(\mathbf{B}_1\mathbf{u}(a) - g_1) + \overline{\mathbf{B}_2\mathbf{v}(b)}(\mathbf{B}_2\mathbf{u}(b) - g_2) = 0 \tag{16}$$

for all admissible $\mathbf{v} \in V$. Clearly, any solution of (16) is also a solution of (15). After substitution of the definitions given above for the differential and algebraic operators, and, for the vector functions, Eq. (16) is transformed into

$$\begin{aligned}
&\int_a^b \{(\overline{v_1} - \overline{v_2'})(w - u') + (\overline{f_1 v_1'} + \overline{f_2 v_1} + \overline{f_3 v_2})(f_1 w' + f_2 w + f_3 u)\}\mathrm{d}x - \int_a^b (\overline{f_1 v_1'} + \overline{f_2 v_1} + \overline{f_3 v_2}) f_4 \,\mathrm{d}x \\
&+ |\varepsilon_1|^2 \overline{v_1(a)} w(a) + \overline{\varepsilon_1}\varepsilon_2 \overline{v_1(a)} u(a) + \overline{\varepsilon_2}\varepsilon_1 \overline{v_2(a)} w(a) + |\varepsilon_2|^2 \overline{v_2(a)} u(a) - \overline{\varepsilon_1}\varepsilon_3 \overline{v_1(a)} - \overline{\varepsilon_2}\varepsilon_3 \overline{v_2(a)} \\
&+ |\varsigma_1|^2 \overline{v_1(b)} w(b) + \overline{\varsigma_1}\varsigma_2 \overline{v_1(b)} u(b) + \overline{\varsigma_2}\varsigma_1 \overline{v_2(b)} w(b) + |\varsigma_2|^2 \overline{v_2(b)} u(b) - \overline{\varsigma_1}\varsigma_3 \overline{v_1(b)} - \overline{\varsigma_2}\varsigma_3 \overline{v_2(b)} = 0.
\end{aligned} \tag{17}$$

For our least squares finite element analysis, we use real piecewise polynomials ϕ_j ($j = 1, \ldots, N$), as basis functions for both components of the vector function $\mathbf{u}$ in the space V. Thus, the finite element approximation $\tilde{\mathbf{u}}(x) = [\,\tilde{w}(x)\ \tilde{u}(x)\,]^{\mathrm{T}}$ of $\mathbf{u}$ can be represented as

$$\tilde{w}(x) = \sum_{j=1}^{N} w_j \phi_j(x) \quad \text{and} \quad \tilde{u}(x) = \sum_{j=1}^{N} u_j \phi_j(x), \tag{18}$$

where $N = ED + 1$ is the number of nodes required to discretize the domain Ω into a finite element mesh with E finite elements, whose basis functions have degree D.

We define the finite element approximation of $\mathbf{v}(x)$, as $\tilde{\mathbf{v}}(x) = [\,\phi_i(x)\ 0\,]^{\mathrm{T}}$, for $i = 1, \ldots, N$, and substitute it into (17). Also, we substitute into (17) the finite element approximations $\tilde{w}(x)$ and $\tilde{u}(x)$ of $w(x)$ and $u(x)$, respectively. As a result, we obtain the following family of algebraic equations:

$$\begin{aligned}
&\sum_{j=1}^{N} \left\{ \left(\int_a^b \{-\phi_i \phi_j' + \overline{f_1} f_3 \phi_i' \phi_j + \overline{f_2} f_3 \phi_i \phi_j\}\mathrm{d}x \right) u_j \right. \\
&\left. + \left(\int_a^b \{(1 + |f_2|^2)\phi_i \phi_j + |f_1|^2 \phi_i' \phi_j' + \overline{f_1} f_2 \phi_i' \phi_j + f_1 \overline{f_2} \phi_i \phi_j'\}\mathrm{d}x \right) w_j \right\} \\
&- \int_a^b \{\overline{f_1}\phi_i' + \overline{f_2}\phi_i\} f_4 \,\mathrm{d}x + |\varepsilon_1|^2 w_1 \delta_{i1} + \overline{\varepsilon_1}\varepsilon_2 u_1 \delta_{i1} - \overline{\varepsilon_1}\varepsilon_3 \delta_{i1} + |\varsigma_1|^2 w_N \delta_{iN} + \overline{\varsigma_1}\varsigma_2 u_N \delta_{iN} - \overline{\varsigma_1}\varsigma_3 \delta_{iN} = 0
\end{aligned} \tag{19}$$

for $i = 1, \ldots, N$. The symbol δ_{ij} represents the δ Kronecker function. Alternatively, by choosing $\mathbf{v}(x) = [\,0\ \phi_i(x)\,]^{\mathrm{T}}$, for $i = 1, 2, \ldots, N$ and substituting the finite element approximations $\tilde{w}(x)$ and $\tilde{u}(x)$ into (17) a second family of algebraic equations for the unknowns w_j and u_j ($j = 1, 2, \ldots, N$) is obtained:

$$\begin{aligned}
&\sum_{j=1}^{N} \left\{ \left(\int_a^b \{\phi_i' \phi_j' + |f_3|^2 \phi_i \phi_j\}\mathrm{d}x \right) u_j + \left(\int_a^b \{-\phi_i' \phi_j + f_1 \overline{f_3} \phi_i \phi_j' + f_2 \overline{f_3} \phi_i \phi_j\}\mathrm{d}x \right) w_j \right\} \\
&- \int_a^b \overline{f_3} f_4 \phi_i \,\mathrm{d}x + |\varepsilon_2|^2 u_1 \delta_{i1} + \varepsilon_1 \overline{\varepsilon_2} w_1 \delta_{i1} - \overline{\varepsilon_2}\varepsilon_3 \delta_{i1} + |\varsigma_2|^2 u_N \delta_{iN} + \varsigma_1 \overline{\varsigma_2} w_N \delta_{iN} - \overline{\varsigma_2}\varsigma_3 \delta_{iN} = 0
\end{aligned} \tag{20}$$

for $i = 1, \ldots, N$. Notice that in both families, the equations corresponding to $i = 1$ and N contain the complex constants ε_j and ς_j present in the boundary conditions (6) and (7). The above Eqs. (19) and (20), represent an algebraic linear system with $2N$ unknowns (w_j, u_j, for $j = 1, \ldots, N$) and $2N$ equations.

3. Formulation of the MGFEM

In this section, we obtain the mixed Galerkin finite element variational formulation of the BVP (4)–(7). It consists of finding a vector function $\mathbf{u}(x) = [\, w(x)\ u(x)\,]^{\mathrm{T}}$, where $w(x) \in X$ and $u(x) \in H$ such that the weighted residual:

$$(\mathbf{Au} - \mathbf{f}, \mathbf{v}) = \int_a^b \mathbf{v}^*(\mathbf{Au} - \mathbf{f})\mathrm{d}x = 0, \tag{21}$$

holds for all test functions $\mathbf{v}(x) = [\, v_1(x)\ v_2(x)\,]$. Here, the asterisk denotes the conjugate transpose of vector $\mathbf{v}$. The subspaces X and H are generally not the same. For example, $X \subset L_2(0, 1)$ and $H \subset H^1(0, 1)$. Next, we substitute the matrix $\mathbf{A}$ by its definition given by Eq. (12), and the vectors $\mathbf{u}$, $\mathbf{v}$, and $\mathbf{f}$ by their corresponding definitions given in the previous section, respectively. As a consequence, the variational formulation of the MGFEM (21) reduces to

$$\int_a^b \{\overline{v_1}(w - u') + \overline{v_2}(f_1 w' + f_2 u' + f_3 u - f_4)\}\mathrm{d}x = 0. \tag{22}$$

Integrating by parts, the second term in Eq. (22) yields:

$$\int_a^b \{\overline{v_1}(w - u') - \overline{v_2'}(f_1 w + f_2 u) + \overline{v_2}(-f_1' w - f_2' u + f_3 u - f_4)\}\mathrm{d}x + (\overline{v_2} f_1)w(b) - (\overline{v_2} f_1)w(a)$$
$$+ (\overline{v_2} f_2 u)(b) - (\overline{v_2} f_2 u)(a) = 0. \tag{23}$$

The finite element analysis of (23) requires the replacement of the secondary and primary variables by their corresponding finite element approximations, $\tilde{w}(x) \in X_h$ and $\tilde{u}(x) \in H_h$, respectively. In general, the finite element spaces X_h and H_h should consist of element shape functions of unequal degree. In fact as pointed out in [8], a good pair of finite element spaces is H_h=\{set of piecewise linear continuous functions\} and X_h=\{set of piecewise constant functions\}. The reason for this choice is to satisfy the LBB stability condition [6]. However, our main purpose is to apply MGFEM to homogeneous equations of the form (1). It means that the possible source of instability, which is the forcing term, is not present. Thus, piecewise polynomial basis functions $\{\phi_i\}_{i=0}^n$ of the same degree can be used to represent both finite element approximations $\tilde{w}(x)$ and $\tilde{u}(x)$, without affecting the stability of the problem. Thus, we replace w and u in (23) by $\tilde{w}$ and $\tilde{u}$ given by (18). As test functions, we use $\tilde{\mathbf{v}}(x) = [\, \phi_i(x)\ 0\,]^{\mathrm{T}}$ and $\tilde{\mathbf{v}}(x) = [\, 0\ \phi_i(x)\,]^{\mathrm{T}}$, for $i = 1, 2, \ldots, N$, As a consequence, we obtain the following two families of $2N$ algebraic equations for the $2N$ unknowns w_j and u_j:

$$\sum_{j=1}^{N} \left\{ \left(-\int_a^b \phi_i \phi_j' \,\mathrm{d}x \right) u_j + \left(\int_a^b \phi_i \phi_j \,\mathrm{d}x \right) w_j \right\} = 0, \tag{24}$$

$$\sum_{j=1}^{N} \left\{ \left(\int_a^b \{-f_2 \phi_i' - f_2' \phi_i + f_3 \phi_i\}\phi_j \,\mathrm{d}x \right) u_j - \left(\int_a^b \{f_1 \phi_i' + f_1' \phi_i\}\phi_j \,\mathrm{d}x \right) w_j \right\} + \phi_i f_2 u_N \delta_{iN} - \phi_i f_2 u_1 \delta_{i1}$$
$$+ \phi_i f_1 w_N \delta_{iN} - \phi_i f_1 w_1 \delta_{i1} - \int_a^b f_4 \phi_i \,\mathrm{d}x = 0 \tag{25}$$

for $i = 1, \ldots, N$. In the next section, we present the details of the process of construction of the finite element approximations.

4. Generation and assembling of the finite element solution

The algebraic linear systems with $2N$ equations and $2N$ unknowns obtained in the previous section for MGFEM and LSFEM are denoted as

$$\mathbf{K\tilde{u}} = \mathbf{l}, \tag{26}$$

where $\mathbf{K}$ is a complex block-banded square matrix of order $2N$ commonly called stiffness matrix, $\mathbf{l}$ is a complex vector with $2N$ components also called load vector, and $\tilde{\mathbf{u}}$ is the unknown vector given by

$$\tilde{\mathbf{u}} = [\, w_1 \; u_1 \; w_2 \; u_2 \; \ldots \; w_N \; u_N \,]^{\mathrm{T}}. \tag{27}$$

A convenient definition of the stiffness matrix $\mathbf{K}$ is obtained by alternating the positions of the unknonws w_i and u_i inside the unknown vector $\tilde{\mathbf{u}}$ such that a w_j is placed first and then the corresponding u_j follows. In order to construct finite element solutions to BVP (4)–(7), the domain $\Omega = [a, b]$ is divided into E elements, Ω_e, for $e = 1, \ldots, E$. Piecewise polynomial basis are defined from element shape functions $\psi_j^e(\xi)$ defined as lagrange interpolating polynomials on a natural coordinate system ($-1 \le \xi \le 1$) with degree $(\psi_j^e) = D \in \mathbb{N}$. Then, the linear system (26) can be locally computed block by block and then assembled element by element as

$$\sum_{e=1}^{E} \mathbf{K}^e \tilde{\mathbf{u}} = \sum_{e=1}^{E} \mathbf{l}^e. \tag{28}$$

Therefore, the family of algebraic equations (19) and (20) for the LSFEM can be written in terms of the finite elements $\Omega_1, \Omega_2, \ldots, \Omega_E$ as follows:

$$\begin{aligned}
&\sum_{e=1}^{E}\sum_{j=1}^{D+1}\left\{\left(\int_{\Omega_e}\{-\psi_i^e\psi_j^{e'} + \overline{f_1}f_3\psi_i^{e'}\psi_j^e + \overline{f_2}f_3\psi_i^e\psi_j^e\}\mathrm{d}\Omega_e\right)u_j^e\right.\\
&\left. + \left(\int_{\Omega_e}\{(1+|f_2|^2)\psi_i^e\psi_j^e + |f_1|^2\psi_i^{e'}\psi_j^{e'} + \overline{f_1}f_2\psi_i^{e'}\psi_j^e + f_1\overline{f_2}\psi_i^e\psi_j^{e'}\}\mathrm{d}\Omega_e\right)w_j^e\right\}\\
&- \sum_{e=1}^{E}\int_{\Omega_e}\{\overline{f_1}\psi_i^{e'} + \overline{f_2}\psi_i^e\}f_4\,\mathrm{d}\Omega_e + |\varepsilon_1|^2 w_1^1\delta_{i1} + \overline{\varepsilon_1}\varepsilon_2 u_1^1\delta_{i1} - \overline{\varepsilon_1}\varepsilon_3\delta_{i1} + |\varsigma_1|^2 w_{D+1}^E\delta_{iN}\\
&+ \overline{\varsigma_1}\varsigma_2 u_{D+1}^E\delta_{iN} - \overline{\varsigma_1}\varsigma_3\delta_{iN} = 0,
\end{aligned} \tag{29}$$

$$\begin{aligned}
&\sum_{e=1}^{E}\sum_{j=1}^{D+1}\left\{\left(\int_{\Omega_e}\{\psi_i^{e'}\psi_j^{e'} + |f_3|^2\psi_i^e\psi_j^e\}\mathrm{d}\Omega_e\right)u_j^e + \left(\int_{\Omega_e}\{-\psi_i^{e'}\psi_j^e + f_1\overline{f_3}\psi_i^e\psi_j^e + f_2\overline{f_3}\psi_i^e\psi_j^e\}\mathrm{d}\Omega_e\right)w_j^e\right\}\\
&- \sum_{e=1}^{E}\int_{\Omega_e}\overline{f_3}f_4\psi_i^e\mathrm{d}\Omega_e + |\varepsilon_2|^2 u_1^1\delta_{i1} + \varepsilon_1\overline{\varepsilon_2}w_1^1\delta_{i1} - \overline{\varepsilon_2}\varepsilon_3\delta_{i1} + |\varsigma_2|^2 u_{D+1}^E\delta_{iN}\\
&+ \varsigma_1\overline{\varsigma_2}w_{D+1}^E\delta_{iN} - \overline{\varsigma_2}\varsigma_3\delta_{iN} = 0
\end{aligned} \tag{30}$$

for $i = 1, \ldots, N$. Similarly, algebraic equations (24) and (25) for the MGFEM can now be written as

$$\sum_{e=1}^{E}\sum_{j=1}^{D+1}\left\{\left(-\int_{\Omega_e}\psi_i^e\psi_j^{e'}\,\mathrm{d}\Omega_e\right)u_j^e + \left(\int_{\Omega_e}\psi_i^e\psi_j^e\,\mathrm{d}\Omega_e\right)w_j^e\right\} = 0, \tag{31}$$

$$\begin{aligned}
&\sum_{e=1}^{E}\sum_{j=1}^{D+1}\left\{\left(\int_{\Omega_e}\{-f_2\psi_i^{e'} - f_2'\psi_i^e + f_3\psi_i^e\}\psi_j^e\,\mathrm{d}\Omega_e\right)u_j^e - \left(\int_{\Omega_e}\{f_1\psi_i^{e'} + f_1'\psi_i^e\}\psi_j^e\,\mathrm{d}\Omega_e\right)w_j^e\right\}\\
&+ \psi_i^e f_2 u_{D+1}^E\delta_{iN} - \psi_i^e f_2 u_1^1\delta_{iN} + \psi_i^e f_1 w_{D+1}^E\delta_{iN} - \psi_i^e f_1 w_1^1\delta_{i1} - \sum_{e=1}^{E}\int_{\Omega_e} f_4\psi_i^e\,\mathrm{d}\Omega_e = 0
\end{aligned} \tag{32}$$

for $i = 1, \ldots, N$.

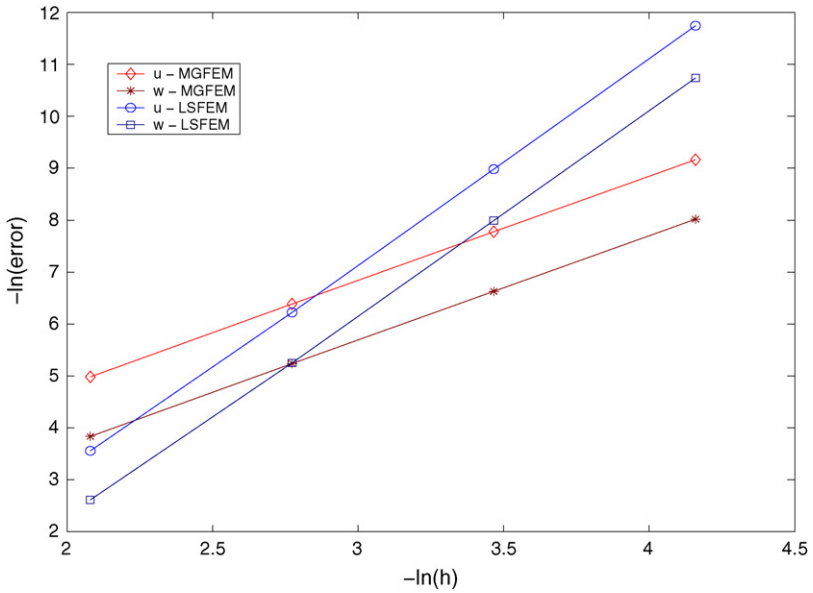

Fig. 1. Rate of convergence for $k = \pi$ and element shape functions of degree $D = 2$.

5. Application to the scattering problem governed by the Helmholtz equation

In this section, the results of the application of LSFEM and MGFEM methods to the BVP (8)–(10), written as the first order system (11), are analyzed. Several experiments are performed defining a uniform mesh with E elements and using Lagrangian element shape functions of various degrees. Then, the absolute error in the L_2 norm is computed for both the primary variable $u = p$ and the secondary variable $w = p'$. The rate of convergence for each method is also obtained by calculating the L_2 absolute error for different values of the distance h between consecutive nodes. The Figs. 1 and 2 correspond to the application of linear regression to the pairs $(-\log(h), -\log(\text{error}))$. It is found that these quantities are linearly related. The slope p of the resulting line is a good approximation to the rate of convergence of the numerical methods.

In Table 1 and Fig. 1, the results for a frequency value $k = \pi$ and Lagrangian element shape functions of degree $D = 2$ are reported. The columns in Table 1 correspond to the number of finite elements E, the L_2 absolute error for the primary variable denoted as error_u, and the L_2 absolute error for the secondary variable denoted as error_w. It is observed that MGFEM approximates the exact solution better than LSFEM for small number of elements. However, as the number of elements is increased LSFEM outperforms MGFEM. In fact, a linear regression analysis on the pairs $(-\log(h), -\log(\text{error}))$ reveals that the order of convergence of LSFEM is $p_u = 3,9419$ with respect to the primary variable u, and, $p_w = 3,9125$ with respect to w. A similar error analysis for the MGFEM leads to orders of convergence $p_u = 2.002$ and $p_w = 2.001$ for u and w, respectively.

The main result of this work is constituted by the above observations regarding the convergence rate of LSFEM when the degree of the element shape functions is increased. For example, regarding the order of convergence, in our previous work [3] we found that to obtain quadratic convergence for $k = \pi$, using linear element shape functions, it

Table 1
L_2 errors for frequency $k = \pi$ and element shape functions of degree $D = 2$

MGFEM			LSFEM		
E	Error_u	Error_w	E	Error_u	Error_w
4	6.8733×10^{-3}	2.1627×10^{-2}	4	2.8559×10^{-2}	7.3353×10^{-2}
8	1.6875×10^{-3}	5.3187×10^{-3}	8	1.9874×10^{-3}	5.2604×10^{-3}
16	4.1993×10^{-4}	1.3220×10^{-3}	16	1.2562×10^{-4}	3.3820×10^{-4}
32	1.0485×10^{-4}	3.2976×10^{-4}	32	7.9434×10^{-6}	2.1713×10^{-5}

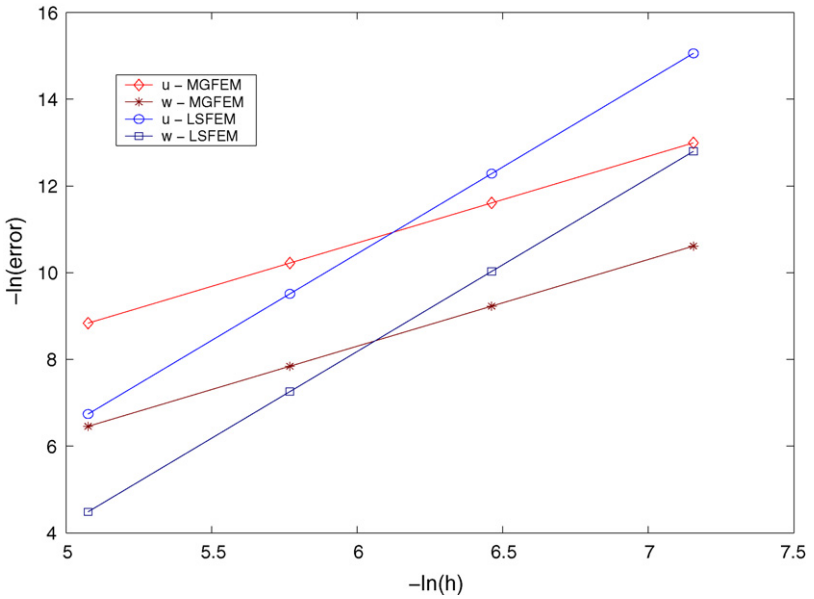

Fig. 2. Rate of convergence for frequency $k = 10$ and element shape functions of degree $D = 2$.

Table 2
L_2 errors for frequency $k = 10$ and element shape functions of degree $D = 2$

MGFEM			LSFEM		
E	Error_u	Error_w	E	Error_u	Error_w
80	1.4562×10^{-4}	1.5731×10^{-3}	80	1.1708×10^{-3}	1.1166×10^{-2}
160	3.6398×10^{-5}	3.9316×10^{-4}	160	7.4595×10^{-5}	7.1265×10^{-4}
320	9.0988×10^{-6}	9.8280×10^{-5}	320	4.6821×10^{-6}	4.4769×10^{-5}
640	2.2746×10^{-6}	2.4569×10^{-5}	640	2.8552×10^{-7}	2.7303×10^{-6}

Table 3
Order of convergence of MGFEM for $k = 10, 20, \ldots, 90$ with element shape functions of degree $D = 5$

	k								
	10	20	30	40	50	60	70	80	90
u-Slope	6.095	6.028	6.069	6.090	6.057	6.08	6.004	6.118	6.146
w-Slope	6.106	6.024	6.065	6.093	6.056	6.072	5.999	6.119	6.142

was necessary to start at least with $E = 50$ elements (51 nodes). In the course of this research (see Table 1), we find that an order of convergence $r = 4$ for $k = \pi$, using element shape functions of degree $D = 2$, can be achieved if we start with only four elements (nine nodes).

Similar results are shown for frequency $k = 10$ and Lagrangian element shape functions of degree $D = 2$, in Table 2 and Fig. 2. It is found that LSFEM maintains a rate of convergence $r = 4$ in both variables. However, in order to attain this order of convergence it is necessary to start with an initial number of elements $E = 80$ (161 nodes). These results

Table 4
Order of convergence of LSFEM for $k = 10, 20, \ldots, 90$ with element shape functions of degree $D = 5$

	k								
	10	20	30	40	50	60	70	80	90
u-Slope	7.537	7.922	7.828	7.844	7.859	7.845	7.831	7.804	7.769
w-Slope	7.980	8.1382	7.898	8.061	7.967	7.904	7.870	7.831	7.781

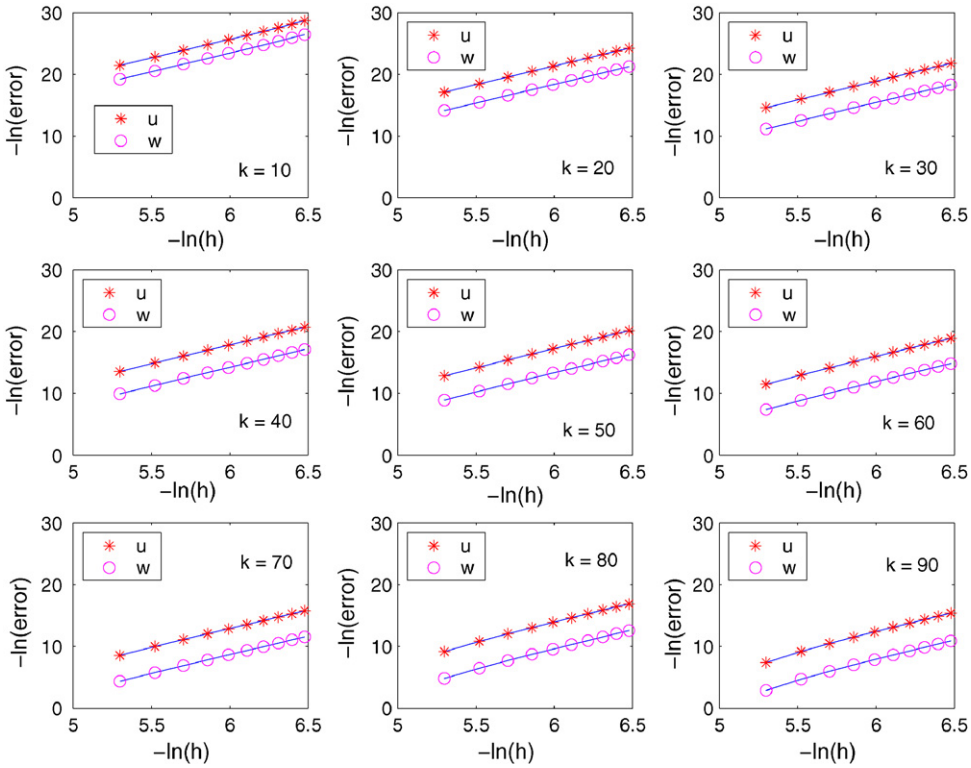

Fig. 3. Computed rates of convergence of MGFEM for $k = 10, 20, \ldots, 90$ with element shape functions of degree $D = 5$.

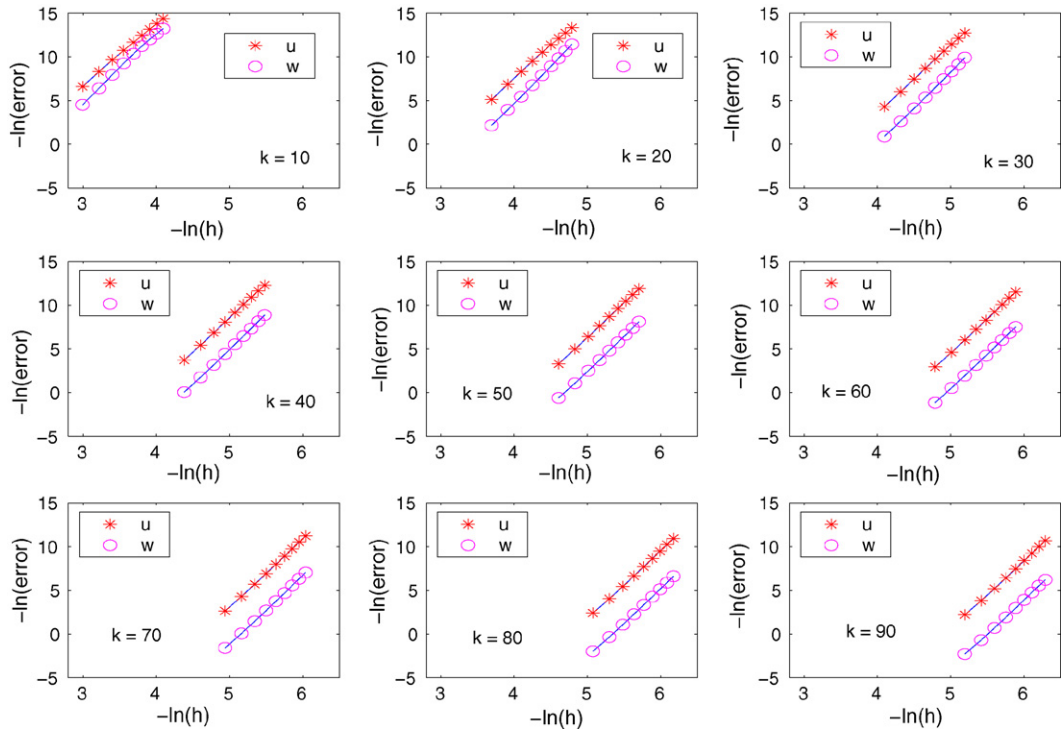

Fig. 4. Computed rates of convergence of LSFEM for $k = 10, 20, \ldots, 90$ with element shape functions of degree $D = 5$.

Table 5
Efficiency comparison between LSFEM and MGFEM for $k = 10$ and $D = 5$

Method	Nodes	Error_u	Error_w	CPU time (s)
$\text{Error}_u < 10^{-6}$				
MGFEM	970	9.902×10^{-7}	1.0695×10^{-5}	20.54
LSFEM	480	9.314×10^{-7}	8.9069×10^{-6}	26.04
$\text{Error}_u < 10^{-7}$				
MGFEM	3100	9.6947×10^{-8}	1.0471×10^{-6}	66.49
LSFEM	850	7.3814×10^{-8}	7.0321×10^{-7}	45.55

follow a pattern observed in [3] for piecewise linear bases. There, to obtain quadratic convergence for $k = 9$, a greater number of elements than those used in a previous experiment, for $k = \pi$, were needed. In fact, a range of elements between 500 and 800 were required. On the other hand, MGFEM did not require as many number of elements to reach the same quadratic order of convergence. In the current experiment, MGFEM also reaches its rate of convergence with much less elements than LSFEM. However in this case ($D = 2$), MGFEM is only of order $r = 2$, while LSFEM is of order $r = 4$ in both variables.

The ability to accurately approximate the physical variables at high frequencies is a desired property of any numerical method applied to scattering phenomena. In the next experiments, we compare the performance of MGFEM and LSFEM for relatively high frequencies using high degree ($D = 5$) element shape functions. Actually, for a range of frequencies $k = 10$–90, the rate of convergence of MGFEM is exhibited in Fig. 3 and Table 3. In these experiments, the initial number of elements used is $E = 40$ (201 nodes) and they are increased by 51 nodes per step, up to 651 nodes. Using this range of elements, the MGFEM achieves a rate of convergence about $r = 6$ for both variables, even for frequencies as high as $k = 90$.

Analogous experiments are performed for LSFEM, the results are shown in Fig. 4 and Table 4. In this case, we need to adjust the number of elements depending on the frequencies (see Fig. 4). For all values of frequencies in the range $k = 10$–90, the order of convergence is about $r = 8$ for element shape functions of degree $D = 5$. Therefore, the convergence rate of LSFEM is also higher than the convergence rate of MGFEM for $D = 5$.

6. Conclusions

In this work, we have found that the approximation of the solution of the scattering problem modelled by the BVP (8)–(10) using LSFEM is possible at low computational cost, even for relatively high frequencies. This conclusion constitutes an important improvement over the results presented in [3]. There, it was found that the application of LSFEM using a piecewise linear basis for moderately high frequencies (e.g. $k = 30$) would require an enormous number of elements. In fact, it was estimated that the number of elements per wavelength required was approximately $5\pi k^2$, for a given frequency k. As a result, the amount of computation, and consequently, the CPU time employed by LSFEM was much greater than the time used by MGFEM to solve the problem for the same frequency. The final conclusion in [3] was that MGFEM had a clear advantage over LSFEM to solve the wave scattering BVP (8)–(10) for relatively high frequencies. Here, we have found that by increasing the degree of the element shape functions in the range $D = 2$–5, the approximation of the primary and the secondary variables using LSFEM is possible at low computational cost. Actually, the number of elements needed to obtain a good approximation dramatically decreases. Thus, CPU time is no longer a disadvantage in the application of LSFEM to scattering problems.

All our numerical tests show that by applying both LSFEM and MGFEM to the scattering problem defined by Eqs. (8)–(10) yield an order of convergence that agrees with the theoretical L_2-estimates of the error [6]; the theoretical error estimate is an order higher than the degree of the element shape polynomials. Moreover, in most of the experiments of the previous section, the LSFEM rate of convergence was greater than the theoretical estimates, and also higher than the MGFEM rate of convergence. For example, Fig. 2 reveals that MGFEM approximation is more precise than LSFEM for a small number of elements. However, as the number of elements is increased, LSFEM approximation is more accurate. This is a a consequence of the higher rate of convergence of LSFEM. In Table 5, the computational cost of each method to attain a specific precision is compared. The second half of the table shows how LSFEM reaches a high predetermined precision in a shorter time, and, with fewer elements than MGFEM. Our final remark is that

LSFEM is well suited for scattering problems at high frequencies ($k = 10$–90) if high degree element shape functions ($D = 2$–5) are used. The extension of this study to two and three-dimensional wave scattering problems is the subject of a work that will be presented in a forthcoming paper.

References

[1] A.K. Aziz, A. Werschulz, On the numerical solution of Helmholtz's equation by the finite element method, SIAM J. Numer. Anal. 17 (1980) 681–686.
[2] R.P. Banaugh, W. Goldsmith, Diffraction of steady acoustic waves by surfaces of arbitrary shape, J. Acoust. Soc. Am. 35 (1963) 1590–1601.
[3] C. Cadenas, V. Villamizar, Comparison of least squares FEM, mixed galerkin FEM and an implicit FDM applied to acoustic scattering, Appl. Numer. Anal. Comput. Math. 1 (2004) 128–139.
[4] G.F. Carey, Y. Shen, Convergence studies of least-squares finite element for first-order systems, Commun. Appl. Numer. Meth. 5 (1989) 427–434.
[5] F. Ihlenburg, Finite Element Analysis of Acoustic Scattering, Springer-Verlag, New York, 1998.
[6] B. Jiang, The Least-squares Finite Element Method: Theory and Applications in Computational Fluid Dynamics and Electromagnetics, Springer-Verlag, New York, 1998.
[7] J.D. Logan, Applied Mathematics, 2nd ed., Wiley-Interscience, 1997.
[8] J.E. Roberts, J.M. Thomas, Mixed and hybrid methods, in: P.G. Ciarlet, J.L. Lions (Eds.), Handbook of Numerical Analysis, vol. II. Finite Element Methods, North Holland, Amsterdam, 1991, pp. 523–639.
[9] A. Taflove, M.E. Brodwin, Numerical solution of steady-state electromagnetic scattering problems using the time-dependent Maxwell's equations, IEEE Trans. Microwave Theory Technol. 23 (1975) 623–630.
[10] A. Taflove, S.C. Hagnes, Computational electrodynamics, in: The Finite-difference Time-domain Method, 2nd ed., Artech House, 2000.
[11] V. Villamizar, O. Rojas, Time-dependent numerical method with boundary-conforming curvilinear coordinates applied to wave interactions with prototypical antennas, J. Comput. Phys. 177 (2002) 1–36.
[12] L.C. Wrobel, The Boundary Element Method, vol. I. John Wiley, West Sussex, England, 2002.

Available online at www.sciencedirect.com
ScienceDirect
Mathematics and Computers in Simulation 73 (2006) 215–225
MATHEMATICS AND COMPUTERS IN SIMULATION
www.elsevier.com/locate/matcom

Matrix approach to mimetic discretizations for differential operators on non-uniform grids

Orestes Montilla[a,*], Carlos Cadenas[a], José Castillo[b]

[a] *Universidad de Carabobo, FACYT, Dpto. de Matemáticas, Valencia, Carabobo, Venezuela*
[b] *San Diego State University, Computational Science Research Center, San Diego, CA, USA*

Available online 22 August 2006

Abstract

Recent investigations have led to a method based on matrix analysis for the construction of high order discrete, fourth and higher mimetic operators, divergence and gradient. These operators have the same order of accuracy in the interior as well as at the boundary on uniform grids. This paper extends the method to non-uniform staggered grids. Here we present this extension on second-order operators although the method works for any order of accuracy. In addition, the boundary operator that allows the operators to satisfy a discrete analog of the divergence theorem is constructed.

Keywords: Mimetic methods; Discrete operators; Conservative methods; Divergence; Gradient

1. Introduction

Mimetic discretization methods are difference discretizations that retain the symmetry properties of the continuum operators. Approximately two decades ago, the support-operators method was developed by Samarskii et al. (see Refs. [10,11]). This method constructs the discrete operators by requiring that these operators satisfy a discrete analog of Green's Theorem [12]. For a summary of methods related with the construction of mimetic discrete operators, see Refs. [5–8], as well as some of their applications [9,13], consult http://cnls.lanl.gov/ shashkov. Recently, Castillo and Grone in Ref. [3] describe a method to construct mimetic discretizations which are high-order approximations of the divergence and gradient operators on uniform grids in 1D. In this article, the Castillo–Grone method, which is based on matrix analysis, is extended to construct mimetic discrete operators on non-uniform, one-dimensional staggered grids. This is achieved through the introduction of a basis function family, which will lead to a new way of finding the Vandermonde matrices that are used to obtain the discrete gradient and divergence operators.

This paper will discuss how to determine these Vandermonde, matrices, obtaining a different way of calculating the operators presented in the Castillo–Grone paper [3]. Then the formulas are generalized to non-uniform grids and the method is illustrated by presenting the second-order operators. This method can be used to find mimetic discrete operators for any order.

In Section 2 we present a short introduction to the methodology of Castillo and Grone. Similarly, in Section 3, we describe the new test functions to obtain the Vandermonde matrices for the discrete divergence and gradient operator.

* Corresponding author.
E-mail addresses: omontila@uc.edu.ve (O. Montilla), ccadenas@uc.edu.ve (C. Cadenas), castillo@myth.sdsu.edu (J. Castillo).

0378-4754/$32.00
doi:10.1016/j.matcom.2006.06.025

Then, in Section 4, the discrete operators, divergence and gradient, in non-uniform grids are calculated using the Vandermonde matrices obtained in Section 3 and the methodology described in Section 2. In addition, the boundary operators satisfying the integration by parts formula are determined. Finally, in Section 5, some conclusions about the results of this work are presented.

2. Preliminaries

Let the domain of variable x be the interval $x_1 \leq x \leq x_{N+1}$. We split this interval into $N+1$ nodes to generate a non-uniform grid with N cells. We identify the nodes by $x_i, i = 1, \ldots, N+1$ and cells by $x_{i+(1/2)}$, which is the midpoint between x_i and x_{i+1}. On this staggered grid, two functions for discrete arguments are defined, the first one is a nodal discretization, where the values of the function correspond to the nodes, the second type of function is cell-valued discretization, where the values of the function correspond to the cells. In Fig. 1, we show the non-uniform staggered grid and grid functions, v and f, which are nodal and cell-valued functions, respectively. The method developed by Castillo and Grone constructs the discrete operators by solving the following system of linear equations:

$$\mathbf{Ma} = \mathbf{r}, \tag{1}$$

where $\mathbf{M}$ is a block matrix, with Vandermonde matrices and identities matrices as its entries, $\mathbf{a}$ the vector of unknown variables, and $\mathbf{r}$ is a vector that is determined by the mimetic conditions. The vector of unknown variables $\mathbf{a}$ leads to k order mimetic differential operators (for details see Ref. [3]).

The procedure to costruct a mimetic operator of high order starts with a mimetic operator that is high order in the interior but not at the boundaries [3]. This operator, represented by the matrix $\mathbf{S}$, is easily constructed via Lagrange interpolation [5]. This matrix is then modified by replacing the upper left corner by a matrix A formed with the entries of the vector $\mathbf{a}$, i.e., the solution to the systems of equations just mentioned. We can summarize the desired properties of our mimetic matrix as follow:

- $\mathbf{S}$ has zero row sums. Equivalently, $\mathbf{S}e = 0$ where $e = (1, 1, \ldots, 1)^t$,
- $\mathbf{S}$ has column sums $-1, 0, \ldots, 0, 1$. Equivalently, $e^t\mathbf{S} = (-1, 0, 0, \ldots, 0, 1)$,
- $\mathbf{S}$ is banded (we let b denote the bandwith of $\mathbf{S}$),
- $\mathbf{S}$ has a "Toeplitz" type structure on the interior rows, and is defined independently of N, the number of grid points,
- $\mathbf{S}$ is centro-skew-symmetric.

3. Test functions and Vandermonde matrices

In the following sections, a formula is found to compute the Vandermonde matrices that will form the systems of linear equations that need to be solved in order to construct mimetic divergence and gradient operators. These formulas are different from those given by Castillo–Grone [3]. The key to obtaining such results relies on choosing appropriate test functions v and f. First of all, we must assume functions v and f are discretizable on nodes and cells, respectively. On a staggered grid, given a continuous function in 1D, it is possible to find for f', the derivative of f, two discrete operators: divergence and gradient.

3.1. Vandermonde matrices for divergence operators

To obtain the mathematical expression of the Vandermonde matrices for the divergence operator, the procedure presented in Ref. [2] is used in a general manner. First, the v function is selected in the nodal function space, and the divergence operator is calculated in cells near the left boundary and is expressed as a linear combination of v in the nodes:

$$(\mathcal{D}_A(\mathbf{v}))_{i+(1/2)} = \sum_{j=1}^{3k/2} a_{ij}\mathbf{v}_j = v'(x_{i+(1/2)}); \quad i = 1, 2 \ldots k, \tag{2}$$

where $\mathcal{D}_A$ is the divergence operator, which acts in the boundary points, $\mathbf{v}_j = v(x_j)$ and the Castillo–Grone methodology demands that if $\mathcal{D}$ is kth order then A is $k \times \frac{3k}{2}$.

The matrix form is

$$\begin{pmatrix} (\mathcal{D}(\mathbf{v}))_{3/2} \\ (\mathcal{D}(\mathbf{v}))_{5/2} \\ \vdots \\ (\mathcal{D}(\mathbf{v}))_{i+(1/2)} \\ \vdots \\ (\mathcal{D}(\mathbf{v}))_{k+(1/2)} \end{pmatrix} = \begin{pmatrix} a_{11} & a_{12} & \cdots & a_{1(3k/2)} \\ a_{21} & a_{22} & \cdots & a_{2(3k/2)} \\ \vdots & \vdots & \vdots & \vdots \\ a_{(k-1)1} & a_{(k-1)2} & \cdots & a_{(k-1)(3k/2)} \\ a_{k1} & a_{k2} & \ldots & a_{k(3k/2)} \end{pmatrix} \begin{pmatrix} \mathbf{v}_1 \\ \mathbf{v}_2 \\ \vdots \\ \mathbf{v}_{(3k/2)-1} \\ \mathbf{v}_{3k/2} \end{pmatrix}. \tag{3}$$

The objective is to obtain approximations of order k to the derivative, i.e., approximations that are exact for every polynomial of degree less than or equal to k but not to $k+1$. For this, without loss of generality, the following polynomials are selected:

$$v_{i,n}(x) = (x - x_{i+(1/2)})^n, \quad \text{where } n = 0, 1, \ldots, k. \tag{4}$$

Now, the evaluation of Eq. (4) in Eq. (2) is presented for each n.
If $n = 0$, $v_{i,0}(x) \equiv 1$, and $v'_{i,0}(x) = 0$, then

$$v'_{i,0}(x_{i+(1/2)}) = 0 \Rightarrow \sum_{j=1}^{3k/2} a_{ij}\mathbf{v}_j = 0 \Rightarrow \sum_{j=1}^{3k/2} a_{ij} = 0; \quad i = 1, 2, \ldots, k. \tag{5}$$

This equation represents the condition of row sums [3].
If $n = 1$, $v_{i,1}(x) = x - x_{i+(1/2)}$; $\quad i = 1, 2, \ldots, k$, then $v'_{i,1}(x) = 1$.
Using the analogous procedure for $n = 0$, we have

$$v'_{i,1}(x_{i+(1/2)}) = 1 \Rightarrow \sum_{j=1}^{3k/2} a_{ij}\mathbf{v}_j = 1 \Rightarrow \sum_{j=1}^{3k/2} a_{ij}(x_j - x_{i+(1/2)}) = 1; \quad i = 1, 2, \ldots, k. \tag{6}$$

Similarly for $n \geq 2$, we get

$$(\mathcal{D}_A(\mathbf{v}))_{i+(1/2)} = \sum_{j=1}^{3k/2} a_{ij}(x_j - x_{i+(1/2)})^n = 0; \quad i = 1, 2, \ldots, k. \tag{7}$$

Using the Kronecker's delta, Eqs. (5)–(7) are expressed as follows:

$$\sum_{j=1}^{3k/2} a_{ij}(x_j - x_{i+(1/2)})^n = \delta_{1n}; \quad i = 1, 2, \ldots, k \text{ and } n = 0, 1, 2, \ldots, k, \tag{8}$$

where $\delta_{1n} = \begin{cases} 1, & \text{if } n = 1 \\ 0, & \text{otherwise} \end{cases}$

Therefore the Vandermonde matrix V_i is

$$V_i = V(k; x_1 - x_{i+(1/2)}, x_2 - x_{i+(1/2)}, \ldots, x_{3k/2} - x_{i+(1/2)}); \quad i = 1, 2, \ldots, k, \tag{9}$$

where

$$V(k; x_1, \ldots, x_n) = \begin{bmatrix} 1 & \cdots & 1 \\ x_1 & \cdots & x_n \\ \vdots & \cdots & \vdots \\ x_1^k & \cdots & x_n^k \end{bmatrix}. \tag{10}$$

In the cases of uniform grids $x_i = ih$ and $x_{i+(1/2)} = \frac{(2i+1)h}{2}$, Eq. (8) is transformed in the following equation:

$$\sum_{j=1}^{3k/2} a_{ij}(2i+1-2j) = -\frac{2^n}{h^n}\delta_{1n}. \tag{11}$$

Since $\frac{2^n}{h^n}\delta_{1n} = 0, \forall n \neq 1$, then Eq. (11) can be written as

$$\sum_{j=1}^{3k/2} a_{ij}(2i+1-2j)^n = -\frac{2}{h}\delta_{1n}; \quad i = 1, 2, \ldots, k \text{ and } n = 0, 1, 2, \ldots, k. \tag{12}$$

From this equation, the Vandermonde matrices for the uniform case are obtained:

$$V_1 = V(k; 1, -1, -3, \ldots, 3-3k), \qquad V_2 = V(k; 3, 1, -1, \ldots, 5-3k),$$
$$V_3 = V(k; 5, 3, 1, \ldots, 7-3k), \ \ldots \ V_k = V(k; 2k-1, 2k-3, \ldots, 1-k), \tag{13}$$

where k Vandermonde matrices are necessary to construct the $\mathbf{M}$ matrix [3]. We can write the above matrices in a compact form:

$$V_i = V(k; 2i-1, 2i-3, \ldots, 2i+1-3k); \quad i = 1, 2, \ldots, k. \tag{14}$$

This result is identical to the one obtained in Ref. [3] for $k = 4$.

Starting from the right side of Eq. (12), the vector $\mathbf{r} = (\mathbf{c}\ \mathbf{c}\ \mathbf{c} \cdots \mathbf{d})^t$ in Eq. (1) is obtained, where $\mathbf{c} = \left(0, -\frac{2}{h}, 0, \ldots, 0\right)^t$ and $\mathbf{d} = (-1, 0, 0, \ldots, 0, 0) \in \mathbb{R}^{3k/2}$ are set to satisfy the column sums condition [3]. This completes the system of Eq. (1) as promised.

3.2. Vandermonde matrices for gradient operator

The construction of the gradient operator follows the one for the divergence operator, but the first one is a nodal grid function while the second one is a cell-valued grid function. That is to say, the respective domains are the center cell and boundary nodes of the grid. Due to this difference, we assume an extended cell-valued discretization on a staggered non-uniform grid, to incorporate boundary nodes to the vector $\mathbf{f}$, and obtain the vector $\hat{\mathbf{f}}$.

Now, if A is a matrix whose dimensions are $k \times \frac{3k}{2}$, the gradient operator on i node can be written as a linear combination of function elements, $\hat{\mathbf{f}} = \{\mathbf{f}_1, \mathbf{f}_{3/2}, \ldots\}$:

$$(\mathcal{G}(\mathbf{f}))_i = a_{i1}\mathbf{f}_1 + \sum_{j=2}^{3k/2} a_{ij}\mathbf{f}_{j-(1/2)}, \quad i = 1, 2, \ldots, k. \tag{15}$$

We propose the family of test functions for the discrete gradient operator:

$$f_{i,n}(x) = (x - x_i)^n, \quad \text{where } n = 0, 1, \ldots, k. \tag{16}$$

In the same way as with the divergence test functions (8), we obtain the formula to calculate:

$$(\mathcal{G}(\mathbf{f}))_i = a_{i1}(x_1 - x_i)^n + \sum_{j=2}^{3k/2} a_{ij}(x_{j-(1/2)} - x_i)^n = \delta_{1n}; \quad i = 1, 2, \ldots, k, \tag{17}$$

where n is valued between 0 and k. The right side of the equation referred before as *Kronecker's delta*, is only not zero for $n = 1$.

In uniform grids, Eq. (17) takes the form:

$$(\mathcal{G}(\mathbf{f}))_i = 2^n a_{i1}(i-1)^n + \sum_{j=2}^{3k/2} a_{ij}(2i+1-2j)^n = \frac{-2}{h}\delta_{1n}; \tag{18}$$

where $i = 1, 2, \ldots, k$ and $n = 0, 1, 2, \ldots, k$.

This equation is similar to Eq. (8); both possess the same right side and summations only differing in the first term. This indicates that the vector **c**, that is part of **r** has the same structure for the divergence operator as for the gradient operator. This is not zero if and only if $n = 1$.

Therefore from Eq. (17) we can obtain the elements of the Vandermonde matrix V_i. These elements are as follows:

$$V_i = V(k; x_1 - x_i, x_{3/2} - x_i, \ldots, x_{(3k-1)/2} - x_i); \quad i = 1, 2, \ldots, k. \tag{19}$$

Using the same procedure as for the divergence operator on uniform grids and Eq. (18), we obtain

$$V_i = V(k; 2i - 2, 2i - 3, 2i - 5, \ldots, 2i + 1 - 3k); \quad i = 1, 2, \ldots, k. \tag{20}$$

Here each one of these matrices has $\frac{3k}{2}$ entries.

The explicit form of these k matrices are:

$$V_1 = V(k; 0, -1, -3, -5, \ldots, 3 - 3k), \qquad V_2 = V(k; 2, 1, -1, \ldots, 5 - 3k),$$
$$V_3 = V(k; 4, 3, 1, \ldots, 7 - 3k), \ \ldots \ V_k = V(k; 2k - 2, 2k - 3, 2k - 5, \ldots, 1 - k). \tag{21}$$

In the same way as for the construction of the divergence operator, we use these Vandermonde matrices to build **M** that is part of the system (1) which will give us our gradient operator.

4. Second-order discrete operator on non-uniform grids

In this section, divergence and gradient mimetic operators on non-uniform staggered grids are presented. Using the procedure described in Section 2 with the Vandermonde matrices obtained in Sections 3.1 and 3.2, the operators of divergence and gradient for $k = 2$ are calculated. Also, the boundary operator that satisfies an equivalent discrete integration by parts formula is obtained.

4.1. Mimetic divergence

Rows of the divergence operator use the classic centered approximation of the derivative [12] of second-order, which is

$$\left(\frac{dv}{dx}\right)_{i+(1/2)} = \frac{v_{i+1} - v_i}{x_{i+1} - x_i}. \tag{22}$$

Using (22) and Castillo–Grone methodology with $k = 2$, a discrete divergence operator is obtained; it is second-order in inner nodes as in the boundary. In this case, the minimum number of cells is $N = 5$. So, the divergence operator has five rows and six columns. Therefore, the mimetic canonical matrix for the divergence $\mathbf{S}_{\mathcal{D}}$ on non-uniform staggered grids is the following

$$\mathbf{S}_{\mathcal{D}} = \begin{pmatrix} -\frac{1}{x_2 - x_1} & \frac{1}{x_2 - x_1} & 0 & 0 & 0 & 0 \\ 0 & -\frac{1}{x_3 - x_2} & \frac{1}{x_3 - x_2} & 0 & 0 & 0 \\ 0 & 0 & -\frac{1}{x_4 - x_3} & \frac{1}{x_4 - x_3} & 0 & 0 \\ 0 & 0 & 0 & -\frac{1}{x_5 - x_4} & \frac{1}{x_5 - x_4} & 0 \\ 0 & 0 & 0 & 0 & -\frac{1}{x_6 - x_5} & \frac{1}{x_6 - x_5} \end{pmatrix}. \tag{23}$$

Let $AA' \in \mathbb{R}^{2\times 3}$ be the necessary matrices to calculate the divergence near the left and right boundaries, respectively, so that at the end we have an operator with the same order of accuracy in the interior as well as at the boundary. Let

the divergence operator $\mathcal{D}(A, A')$ be

$$\mathcal{D}(A, A') = \begin{pmatrix} a_{11} & a_{12} & a_{13} & 0 & 0 & 0 \\ a_{21} & a_{22} & a_{23} & 0 & 0 & 0 \\ 0 & 0 & -\dfrac{1}{x_4 - x_3} & \dfrac{1}{x_4 - x_3} & 0 & 0 \\ 0 & 0 & 0 & a'_{11} & a'_{12} & a'_{13} \\ 0 & 0 & 0 & a'_{21} & a'_{22} & a'_{23} \end{pmatrix}. \tag{24}$$

For $k = 2$, two Vandermonde matrices are needed to form the matrix (M), and these are obtained from the coefficients of the formula (9). These matrices are

$$V_1 = V(2; x_1 - x_{3/2}, x_2 - x_{3/2}, x_3 - x_{3/2}) \quad \text{and} \quad V_2 = V(2; x_1 - x_{5/2}, x_2 - x_{5/2}, x_3 - x_{5/2}).$$

Using the methodology presented in the preliminaries section and substituting the middle points by $x_{3/2} = \frac{x_1+x_2}{2}$ and $x_{5/2} = \frac{x_2+x_3}{2}$, we have

$$\mathbf{M} = \begin{pmatrix} 1 & 1 & 1 & 0 & 0 & 0 \\ \dfrac{x_1}{2} - \dfrac{x_2}{2} & \dfrac{x_2}{2} - \dfrac{x_1}{2} & x_3 - \dfrac{x_1}{2} - \dfrac{x_2}{2} & 0 & 0 & 0 \\ \left(\dfrac{x_1}{2} - \dfrac{x_2}{2}\right)^2 & \left(\dfrac{x_2}{2} - \dfrac{x_1}{2}\right)^2 & \left(x_3 - \dfrac{x_1}{2} - \dfrac{x_2}{2}\right)^2 & 0 & 0 & 0 \\ 0 & 0 & 0 & 1 & 1 & 1 \\ 0 & 0 & 0 & x_1 - \dfrac{x_2}{2} - \dfrac{x_3}{2} & \dfrac{x_2}{2} - \dfrac{x_3}{2} & \dfrac{x_3}{2} - \dfrac{x_2}{2} \\ 0 & 0 & 0 & \left(x_1 - \dfrac{x_2}{2} - \dfrac{x_3}{2}\right)^2 & \left(\dfrac{x_2}{2} - \dfrac{x_3}{2}\right)^2 & \left(\dfrac{x_3}{2} - \dfrac{x_2}{2}\right)^2 \\ 1 & 0 & 0 & 1 & 0 & 0 \\ 0 & 1 & 0 & 0 & 1 & 0 \\ 0 & 0 & 1 & 0 & 0 & 1 \end{pmatrix},$$

and $\mathbf{r} = (0\ 1\ 0\ 0\ 1\ 0\ -1\ 0\ 1)^t$. The system $\mathbf{Ma} = \mathbf{r}$ is not compatible, so rows two and five are eliminated to form a new linear system of equations and the solution $\hat{A}$ to the new system $\mathbf{M_w}\hat{a} = \hat{\mathbf{r}}$ is

$$\hat{A} = \begin{pmatrix} -1 & 1 & 0 \\ 0 & -1 & 1 \end{pmatrix}.$$

This solution is the same as the one for the uniform case [3]. It is clear that $\hat{a}$ vector has elements of $\hat{A}$. Now we calculate $\hat{\Lambda}$ and subsequently $\hat{Q}$, obtaining

$$\hat{\Lambda} = \begin{pmatrix} x_2 - x_1 \\ x_3 - x_2 \end{pmatrix}, \qquad \hat{Q} = \begin{pmatrix} x_2 - x_1 & 0 \\ 0 & x_3 - x_2 \end{pmatrix},$$

where $\hat{\Lambda}$ matrix has diagonal elements of the weight matrix $\hat{Q}$, which is the upper left block matrix of Q. Then we calculate $A = \hat{A}\hat{Q}^{-1}$. The result is

$$A = \begin{pmatrix} \dfrac{-1}{x_2 - x_1} & \dfrac{1}{x_2 - x_1} & 0 \\ 0 & \dfrac{-1}{x_3 - x_2} & \dfrac{1}{x_3 - x_2} \end{pmatrix}.$$

The A matrix necessary to modify the canonical matrix, $\mathbf{S}_{\mathcal{D}}$ (23), has the elements eliminated, i.e., $\mathcal{D}(A, A') = \mathbf{S}_{\mathcal{D}}$. If a uniform grid is used, this matrix is the same obtained by Castillo and Yasuda in Ref. [4].

4.2. Mimetic gradient

The same procedure utilized for calculating the divergence operator works for the gradient operator. For a non-uniform staggered grid with $N = 5$, the gradient operator has six rows and seven columns. This is because the boundary is incorporated. The canonical matrix $\mathbf{S}_{\mathcal{G}}$ is constructed utilizing the approximation of order one in the inner nodes as in the boundary. This canonical matrix is

$$\mathbf{S}_{\mathcal{G}} = \begin{pmatrix} \frac{-2}{x_{3/2}-x_1} & \frac{2}{x_{3/2}-x_1} & 0 & 0 & 0 & 0 & 0 \\ 0 & \frac{-1}{x_{5/2}-x_{3/2}} & \frac{1}{x_{5/2}-x_{3/2}} & 0 & 0 & 0 & 0 \\ 0 & 0 & \frac{-1}{x_{7/2}-x_{5/2}} & \frac{1}{x_{7/2}-x_{5/2}} & 0 & 0 & 0 \\ 0 & 0 & 0 & \frac{-1}{x_{9/2}-x_{7/2}} & \frac{1}{x_{9/2}-x_{7/2}} & 0 & 0 \\ 0 & 0 & 0 & 0 & \frac{-1}{x_5-x_{9/2}} & \frac{1}{x_5-x_{9/2}} & 0 \\ 0 & 0 & 0 & 0 & 0 & \frac{-2}{x_6-x_{11/2}} & \frac{2}{x_6-x_{11/2}} \end{pmatrix}. \tag{25}$$

The substitution of matrices A and A' in $\mathbf{S}_{\mathcal{G}}$ leads to the matrix $\mathcal{G}(A)$:

$$\mathcal{G}(A) = \begin{pmatrix} a_{11} & a_{12} & a_{13} & 0 & 0 & 0 & 0 \\ a_{21} & a_{22} & a_{23} & 0 & 0 & 0 & 0 \\ 0 & 0 & \frac{-1}{x_{7/2}-x_{5/2}} & \frac{1}{x_{7/2}-x_{5/2}} & 0 & 0 & 0 \\ 0 & 0 & 0 & \frac{-1}{x_{9/2}-x_{7/2}} & \frac{1}{x_{9/2}-x_{7/2}} & 0 & 0 \\ 0 & 0 & 0 & 0 & a'_{11} & a'_{12} & a'_{13} \\ 0 & 0 & 0 & 0 & a'_{21} & a'_{22} & a'_{23} \end{pmatrix}. \tag{26}$$

The Vandermonde matrices (19) necessary to generate $\mathbf{M}$ are

$$V_1 = V(2; 0, x_{3/2}-x_1, x_{5/2}-x_1), \qquad V_2 = V(2; x_1-x_2, x_{3/2}-x_2, x_{5/2}-x_2)$$

The linear system has the following matrix of coefficients $\mathbf{M}$:

$$\mathbf{M} = \begin{pmatrix} 1 & 1 & 1 & 0 & 0 & 0 \\ 0 & x_{3/2}-x_1 & x_{5/2}-x_1 & 0 & 0 & 0 \\ 0 & (x_{3/2}-x_1)^2 & (x_{5/2}-x_1)^2 & 0 & 0 & 0 \\ 0 & 0 & 0 & 1 & 1 & 1 \\ 0 & 0 & 0 & 2x_1-2x_{3/2} & -x_{3/2}+x_1 & x_{5/2}-2x_{3/2}+x_1 \\ 0 & 0 & 0 & (2x_1-2x_{3/2})^2 & (-x_{3/2}+x_1)^2 & (x_{5/2}-2x_{3/2}+x_1)^2 \\ 1 & 0 & 0 & 1 & 0 & 0 \\ 0 & 1 & 0 & 0 & 1 & 0 \\ 0 & 0 & 1 & 0 & 0 & 1 \end{pmatrix}$$

Here the expression $x_2 = 2x_{3/2} - x_1$ is used and $\mathbf{r}$ is the same as the one for the divergence:

$$\mathbf{r} = (0\ 1\ 0\ 0\ 1\ 0\ -1\ 0\ 1)^t.$$

As the system is incompatible, rows two and five of $\mathbf{M}$ are eliminated and the solution to the new system is:

$$a_{11} = \frac{11x_1x_{3/2} - 6x_1^2 - 4x_{3/2}^2 - 3x_{5/2}x_{3/2} + x_{5/2}^2 + x_{5/2}x_1}{4(x_{3/2}^2 - 2x_1x_{3/2} + {x_1}^2)},$$

$$a_{12} = \frac{x_{5/2}^3 + x_{5/2}^2x_1 - 5x_{5/2}x_1^2 + 3x_1^3 - 4x_{5/2}^2x_{3/2} + 8x_{5/2}x_1x_{3/2} - 4x_1^2x_{3/2}}{4(x_{3/2}^2 - 2x_1x_{3/2} + x_1^2)(-x_{5/2} + x_{3/2})}, \qquad a_{13} = \frac{-x_{5/2} + 4x_{3/2} - 3x_1}{4(-x_{5/2} + x_{3/2})},$$

$$a_{21} = \frac{-3x_1x_{3/2} + 3x_{5/2}x_{3/2} - x_{5/2}^2 - x_{5/2}x_1 + 2x_1^2}{4(x_{3/2}^2 - 2x_1x_{3/2} + x_1^2)},$$

$$a_{22} = \frac{-x_{5/2}^3 - x_{5/2}^2x_1 + 5x_{5/2}x_1^2 - 3x_1^3 + 4x_{5/2}^2x_{3/2} - 8x_{5/2}x_1x_{3/2} + 4x_1^2x_{3/2}}{4(x_{3/2}^2 - 2x_1x_{3/2} + x_1^2)(-x_{5/2} + x_{3/2})}, \qquad a_{23} = \frac{3(x_{5/2} - x_1)}{4(-x_{5/2} + x_{3/2})}.$$

To calculate the diagonal matrix $\hat{\Lambda}$, and consequentially $\hat{P}$, we construct the subsystem $\mathbf{M_w}\hat{\mathbf{a}}$, where $\mathbf{M_w}$ is the matrix constructed with the rows deleted from $\mathbf{M}$, and $\hat{\mathbf{a}}$ is the vector which elements are the components of $\hat{A}$. $\hat{P}$ is calculated similarly to $\hat{Q}$ and for this case is the following:

$$\hat{P} = \begin{pmatrix} \dfrac{(-x_{5/2} + x_1)(x_{5/2} - 4x_{3/2} + 3x_1)}{4(x_{3/2} - x_1)} & 0 \\ 0 & \dfrac{(-x_{5/2} + x_1)^2}{4(x_{3/2} - x_1)} \end{pmatrix}.$$

Therefore, the matrix A is

$$A = \begin{pmatrix} \dfrac{x_{3/2} + x_{5/2} - 2x_1}{(x_{3/2} - x_1)(-x_{5/2} + x_1)} & \dfrac{-x_{5/2} + x_1}{(-x_{5/2} + x_{3/2})(x_{3/2} - x_1)} & -\dfrac{x_{3/2} - x_1}{(-x_{5/2} + x_{3/2})(-x_{5/2} + x_1)} \\ -\dfrac{-2x_1 + 3x_{3/2} - x_{5/2}}{(x_{3/2} - x_1)(-x_{5/2} + x_1)} & \dfrac{-x_{5/2} + 4x_{3/2} - 3x_1}{(-x_{5/2} + x_{3/2})(x_{3/2} - x_1)} & \dfrac{3(x_{3/2} - x_1)}{(-x_{5/2} + x_{3/2})(-x_{5/2} + x_1)} \end{pmatrix}.$$

Substituting this result in Eq. (26), we have the discrete gradient operator $\mathcal{G}$ of second-order on the boundary and first-order on inner nodes:

$$\begin{pmatrix} \frac{2x_1 - x_{5/2} - x_{3/2}}{(x_{3/2} - x_1)(x_{5/2} - x_1)} & \frac{x_{5/2} - x_1}{(x_{5/2} - x_{3/2})(x_{3/2} - x_1)} & \frac{-x_{3/2} + x_1}{(x_{5/2} - x_{3/2})(x_{5/2} - x_1)} & 0 & 0 & 0 & 0 \\ \frac{-2x_1 + 3x_{3/2} - x_{5/2}}{(x_{3/2} - x_1)(x_{5/2} - x_1)} & \frac{x_{5/2} - 4x_{3/2} + 3x_1}{(x_{5/2} - x_{3/2})(x_{3/2} - x_1)} & \frac{3x_{3/2} - 3x_1}{(x_{5/2} - x_{3/2})(x_{5/2} - x_1)} & 0 & 0 & 0 & 0 \\ 0 & 0 & \frac{-1}{x_{7/2} - x_{5/2}} & \frac{1}{x_{7/2} - x_{5/2}} & 0 & 0 & 0 \\ 0 & 0 & 0 & \frac{-1}{x_{9/2} - x_{7/2}} & \frac{1}{x_{9/2} - x_{7/2}} & 0 & 0 \\ 0 & 0 & 0 & 0 & \frac{3(x_{11/2} - x_6)}{(x_{9/2} - x_{11/2})(x_{9/2} - x_6)} & \frac{x_{9/2} - 4x_{11/2} + 3x_6}{(x_{9/2} - x_{11/2})(x_{9/2} - x_6)} & \frac{-2x_6 + 3x_{11/2} - x_{9/2}}{(x_{11/2} - x_6)(x_{9/2} - x_6)} \\ 0 & 0 & 0 & 0 & \frac{-x_{11/2} + x_6}{(x_{9/2} - x_{11/2})(x_{9/2} - x_6)} & \frac{x_{9/2} - x_6}{(x_{9/2} - x_{11/2})(x_{11/2} - x_6)} & \frac{2x_6 - x_{11/2} - x_{9/2}}{(x_{11/2} - x_6)(x_{9/2} - x_6)} \end{pmatrix} \tag{27}$$

If $x_1 = 0; x_{3/2} = \frac{h}{2}; x_{5/2} = 3\frac{h}{2}; x_{7/2} = 5\frac{h}{2}; x_{9/2} = 7\frac{h}{2}; x_5 = 4h$, i.e., using a uniform staggered grid, then

$$\mathcal{G} = \frac{1}{h}\begin{pmatrix} \frac{-8}{3} & 3 & \frac{-1}{3} & 0 & 0 & 0 & 0 \\ 0 & -1 & 1 & 0 & 0 & 0 & 0 \\ 0 & 0 & -1 & 1 & 0 & 0 & 0 \\ 0 & 0 & 0 & -1 & 1 & 0 & 0 \\ 0 & 0 & 0 & 0 & -1 & 1 & 0 \\ 0 & 0 & 0 & 0 & \frac{1}{3} & -3 & \frac{8}{3} \end{pmatrix}. \tag{28}$$

This operator is presented by Castillo and Yasuda in Ref. [4], which is second-order everywhere.

4.2.1. Boundary operator

Usually laws of discrete conservation can be expressed in terms of the usual inner product through the equation:

$$(\hat{\mathcal{D}}(\mathbf{v}), \hat{\mathbf{f}}) + (\mathcal{G}^t(\mathbf{v}), \hat{\mathbf{f}}) = (\mathbf{B}\mathbf{v}, \hat{\mathbf{f}}). \tag{29}$$

The right side of this equation contains a matrix **B**, which is the boundary operator. This operator has dimensions $(N+2) \times (N+1)$, for the method of support operators. Its form is quite elementary [4], because the first element is -1, the last 1, and all others are null. This is a natural form of **B** for mimetic discretization since this guarantees that the discrete divergence theorem is satisfied. That is to say, **B** picks up the requirements of global conservation law.

However, as was demonstrated in Ref. [3], if the order of our discrete differential operator is larger than two, it is impossible to obtain a mimetic operator, with the same order of accuracy up to the boundaries, with the standard inner product. So, it is necessary to introduce a generalized inner product (or weighted inner product). If we use definitions given by Castillo and Grone in Ref. [3], we have the following discrete version of the generalized divergence theorem:

$$(\hat{\mathcal{D}}(\mathbf{v}), \hat{\mathbf{f}})_Q + (\mathcal{G}^t(\mathbf{v}), \hat{\mathbf{f}})_P = (\mathbf{B}\mathbf{v}, \hat{\mathbf{f}}). \tag{30}$$

Here, $\hat{\mathcal{D}}$ is the discrete divergence operator extended with two null rows, first and last, and **B** is determined by our discrete analog of the divergence theorem with the weighted inner product. Regrettably, it does not take an elementary form as the one for the usual inner product.This matrix is centro-skew-symmetric in structure [1].

From Eq. (30) we can determine **B** by using the following expression directly:

$$\mathbf{B} = Q\hat{\mathcal{D}} + \mathcal{G}^t P. \tag{31}$$

As we said before, the matrix representing the divergence operator was increased in two rows of zeros (first and last), to make the matrices of the same dimension. The same is done with the weight matrix Q; in this case ones are added in the diagonal. Let us remember that the gradient operator has dimensions $(N+1) \times (N+2)$, the divergence operator with two rows more $\hat{\mathcal{D}}$ has dimensions $(N+2) \times (N+1)$. It is clear that P and Q are centro-symmetric and positive defined matrices. Here we present the extended mimetic divergence operator on non-uniform grids:

$$\hat{\mathcal{D}} = \begin{pmatrix} 0 & 0 & 0 & 0 & 0 & 0 \\ \frac{-1}{x_2 - x_1} & \frac{1}{x_2 - x_1} & 0 & 0 & 0 & 0 \\ 0 & \frac{-1}{x_3 - x_2} & \frac{1}{x_3 - x_2} & 0 & 0 & 0 \\ 0 & 0 & \frac{-1}{x_4 - x_3} & \frac{1}{x_4 - x_3} & 0 & 0 \\ 0 & 0 & 0 & \frac{-1}{x_5 - x_4} & \frac{1}{x_5 - x_4} & 0 \\ 0 & 0 & 0 & 0 & \frac{-1}{x_6 - x_5} & \frac{1}{x_6 - x_5} \\ 0 & 0 & 0 & 0 & 0 & 0 \end{pmatrix}.$$

The weight matrix Q can be expressed with parameters t and T in the first and last element, respectively, in such a way that if we want to obtain a uniform Q, we should take both equally

$$Q = \begin{pmatrix} t(x_{3/2} - x_1) & 0 & 0 & 0 & 0 & 0 & 0 \\ 0 & x_2 - x_1 & 0 & 0 & 0 & 0 & 0 \\ 0 & 0 & x_3 - x_2 & 0 & 0 & 0 & 0 \\ 0 & 0 & 0 & x_4 - x_3 & 0 & 0 & 0 \\ 0 & 0 & 0 & 0 & x_5 - x_4 & 0 & 0 \\ 0 & 0 & 0 & 0 & 0 & x_6 - x_5 & 0 \\ 0 & 0 & 0 & 0 & 0 & 0 & T(x_6 - x_{11/2}) \end{pmatrix}.$$

The weight matrix P for the discrete gradient operator is

$$P = \begin{pmatrix} \frac{(-x_{5/2} + x_1)(x_{5/2} - 4x_{3/2} + 3x_1)}{4(x_{3/2} - x_1)} & 0 & 0 & 0 & 0 & 0 \\ 0 & \frac{(-x_{5/2} + x_1)^2}{4(x_{3/2} - x_1)} & 0 & 0 & 0 & 0 \\ 0 & 0 & x_{7/2} - x_{5/2} & 0 & 0 & 0 \\ 0 & 0 & 0 & x_{9/2} - x_{7/2} & 0 & 0 \\ 0 & 0 & 0 & 0 & \frac{(-x_{9/2} + x_6)^2}{4(x_{11/2} - x_6)} & 0 \\ 0 & 0 & 0 & 0 & 0 & \frac{(-x_{9/2} + x_6)(x_{9/2} - 4x_{11/2} + 3x_6)}{4(x_{11/2} - x_6)} \end{pmatrix}.$$

Calculations give us finally the matrix **B** for non-uniform grids. Subsequently, we exhibit the form of the non-null elements for this matrix:

$$\mathbf{B} = \begin{pmatrix} b_{11} & b_{12} & 0 & 0 & 0 & 0 \\ b_{21} & b_{22} & 0 & 0 & 0 & 0 \\ b_{31} & b_{32} & 0 & 0 & 0 & 0 \\ 0 & 0 & 0 & 0 & 0 & 0 \\ 0 & 0 & 0 & 0 & b_{55} & b_{56} \\ 0 & 0 & 0 & 0 & b_{65} & b_{66} \\ 0 & 0 & 0 & 0 & b_{75} & b_{76} \end{pmatrix} \tag{32}$$

namely:

$$b_{11} = \frac{(x_{5/2} - 4x_{3/2} + 3x_1)(-2x_1 + x_{5/2} + x_{3/2})}{4(x_{3/2} - x_1)^2}, \qquad b_{12} = \frac{(-x_{5/2} + x_1)(2x_1 - 3x_{3/2} + x_{5/2})}{4(x_{3/2} - x_1)^2},$$

$$b_{21} = \frac{4x_{5/2}x_{3/2}^2 - x_{5/2}x_1^2 - 4x_{3/2}^3 + 8x_1x_{3/2}^2 - 8x_{3/2}x_1^2 + x_{5/2}^3 + x_{5/2}^2x_1 - 4x_{3/2}x_{5/2}^2 + 3x_1^3}{4(-x_{5/2} + x_{3/2})(x_{3/2} - x_1)^2},$$

$$b_{22} = \frac{4x_{5/2}x_{3/2}^2 - x_{5/2}x_1^2 - 4x_{3/2}^3 + 8x_1x_{3/2}^2 - 8x_{3/2}x_1^2 + x_{5/2}^3 + x_{5/2}^2x_1 - 4x_{3/2}x_{5/2}^2 + 3x_1^3}{4(x_{5/2} - x_{3/2})(x_{3/2} - x_1)^2},$$

$$b_{31} = \frac{x_{5/2} - 4x_{3/2} + 3x_1}{4(x_{5/2} - x_{3/2})}, \qquad b_{32} = \frac{x_{5/2} - 4x_{3/2} + 3x_1}{4(-x_{5/2} + x_{3/2})}, \qquad b_{55} = \frac{-x_{9/2} + 4x_{11/2} - 3x_6}{4(-x_{9/2} + x_{11/2})},$$

$$b_{56} = \frac{x_{9/2} - 4x_{11/2} + 3x_6}{4(-x_{9/2} + x_{11/2})},$$

$$b_{65} = \frac{-4x_{9/2}x_{11/2}^2 + x_{9/2}x_6^2 + 4x_{11/2}^3 - 8x_6x_{11/2}^2 + 8x_{11/2}x_6^2 + 4x_{9/2}^2x_{11/2} - x_{9/2}^2x_6 - x_{9/2}^3 - 3x_6^3}{4(x_{9/2} - x_{11/2})(x_{11/2} - x_6)^2},$$

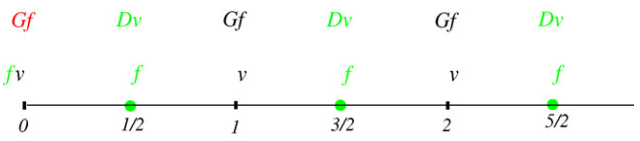

Fig. 1. Staggered grid.

$$b_{66} = \frac{-4x_{9/2}x_{11/2}^2 + x_{9/2}x_6^2 + 4x_{11/2}^3 - 8x_6{x_{11/2}}^2 + 8x_{11/2}{x_6}^2 + 4{x_{9/2}}^2x_{11/2} - {x_{9/2}}^2x_6 - {x_{9/2}}^3 - 3{x_6}^3}{4(-x_{9/2} + x_{11/2})(x_{11/2} - x_6)^2},$$

$$b_{75} = \frac{(-x_{9/2} + x_6)(-2x_6 + 3x_{11/2} - x_{9/2})}{4(x_{11/2} - x_6)^2}, \qquad b_{76} = \frac{(-x_{9/2} + 4x_{11/2} - 3x_6)(-2x_6 + x_{11/2} + x_{9/2})}{4(x_{11/2} - x_6)^2}.$$

We can see that this matrix is centro-skew-symmetric. In accordance with our discretizations, this matrix has dimensions $N + 2$ by $N + 1$.

If we want to compute the respective boundary operator for uniform grids, we should only make appropriate substitutions in the operator above. In this case the obtained **B** operator coincides with the one presented in Ref. [4].

5. Conclusions

Using matrix analysis we have characterized the problem of constructing second-order approximations of the derivative on non-uniform staggered grids that satisfy a global conservation law. Formulas that generate Vandermonde matrices on non-uniform and uniform grids are obtained. This allows us to construct high order approximations for the divergence and gradient on uniform and non-uniform staggered grids in 1D. Contrary to the case of uniform grids, in the case of non-uniform grids, the system of equations for the divergence becomes incompatible. We have calculated the boundary operator **B**, which is needed to satisfy our global conservation law. These results were obtained, using our proposed test functions for divergence and gradient operators. They provide formulas that give the entries of the *Vandermonde matrices*. These matrices play a decisive part in constructing the needed system of equations because they are fundamental in the structuring of the coefficients matrix **M**. Formulas that we have obtained are general because we can use these on uniform grids, smooth non-uniform, and non-smooth, non-uniform grids. In this case, the discrete mimetic divergence operator is second-order everywhere and the discrete mimetic gradient operator is second-order on boundary nodes and first-order on inner nodes.

References

[1] A. Andrew, Centrosymmetric matrices, SIAM Rev. (40) (1998) 697–699.
[2] C. Cadenas, O. Montilla. Generalización de la Matriz de Vandermonde utilizada en la Construcción de Operadores Miméticos Discretos para la Divergencia. Revista INGENIERIA UC, 2004 (submitted for publication).
[3] J. Castillo, R. Grone, A matrix analysis approach to higher-order approximations for divergence and gradients satisfying a global conservation law, SIAM J. Matrix Anal. Appl. 25 (1) (2003) 128–142.
[4] J. Castillo, M. Yasuda, A comparison of two matrix operator formulations for mimetic divergence and gradient discretizations, in: Proceedings of the International Conference on Parallel and Distributed Procesings Techniques and Applications, vol. III, 2003, pp. 1281–1285.
[5] J. Castillo, J. Hyman, M. Shashkov, S. Steinberg, High-order mimetic finite difference methods on nonuniform grids, in: ICOSAHOM 95, Houston, TX, 1996, pp. 347–361.
[6] J. Castillo, J.M. Hyman, M. Shashkov, S. Steinberg, Fourth- and six-order conservative finite difference approximations of the divergence and gradient, Appl. Numer. Math. 37 (2001) 171–187.
[7] J. Hyman, M. Shashkov, Adjoint operators for the natural discretizations of the divergence, gradient, and curl on logically rectangular grids, Appl. Numer. Math. 25 (1997) 413–442.
[8] J. Hyman, M. Shashkov, Approximation of boundary conditions for mimetic finite-difference methods, Comput. Math. Appl. 36 (5) (1998) 79–99.
[9] J. Hyman, M. Shashkov, S. Steinberg, The numerical solution of diffusion problems in strongly heterogeneous non-isotropic materials, J. Comp. Phys. 132 (1997) 130–148.
[10] A. Samarskii, V. Tishkin, A. Favorskii, M. Shashkov, Operational finite-difference schemes, Diff. Eqns. 17 (7) (1981) 854–862.
[11] A. Samarskii, V. Tishkin, A. Favorskii, M. Shashkov, Employment of the reference-operator method in the construction of finite difference analog of tensor operations, Diff. Eqns. 18 (7) (1982) 881–885.
[12] M. Shashkov, Conservative Finite-difference Methods on General Grids, CRC Press, Florida, USA, 1996.
[13] M. Shashkov, S. Steinberg, Solving diffusion equations with rough coefficients in rough grids, J. Comp. Phys. 129 (1996) 383–405.